https://doi.org/10.5194/esd-2021-90
Preprint. Discussion started: 12 November 2021

Earth System Dynamics Discussions
Open Access
EGU

Rapid attribution analysis of the extraordinary heatwave on the Pacific Coast of the US and Canada June 2021

Sjoukje Y. Philip[1,*], Sarah F. Kew[1,*], Geert Jan van Oldenborgh[1,2,†], Faron S. Anslow[3], Sonia I. Seneviratne[4], Robert Vautard[5], Dim Coumou[1,6], Kristie L. Ebi[7], Julie Arrighi[8,9,10], Roop Singh[8], Maarten van Aalst[8,9,11], Carolina Pereira Marghidan[9], Michael Wehner[12], Wenchang Yang[13], Sihan Li[14], Dominik L. Schumacher[4], Mathias Hauser[4], Rémy Bonnet[5], Linh N. Luu[1], Flavio Lehner[15,16], Nathan Gillett[17], Jordis Tradowsky[18,19], Gabriel A. Vecchi[13,20], Chris Rodell[21], Roland B. Stull[21], Rosie Howard[21], and Friederike E. L. Otto[14]

[1]Royal Netherlands Meteorological Institute (KNMI), De Bilt, The Netherlands
[*]These authors contributed equally to this work.
[2]Atmospheric, Oceanic and Planetary Physics, University of Oxford, UK
[†]deceased, 12 October 2021
[3]Pacific Climate Impacts Consortium, University of Victoria, Victoria, V8R4J1, Canada
[4]Institute for Atmospheric and Climate Science, Department of Environmental Systems Science, ETH Zurich, Zurich, Switzerland
[5]Institut Pierre-Simon Laplace, CNRS, Sorbonne Université, Paris, France
[6]Institute for Environmental Studies (IVM), VU Amsterdam, The Netherlands
[7]Center for Health and the Global Environment, University of Washington, Seattle WA, USA
[8]Red Cross Red Crescent Climate Centre, The Hague, the Netherlands
[9]Faculty of Geo-Information Science and Earth Observation (ITC), University of Twente, Enschede, the Netherlands
[10]Global Disaster Preparedness Center, American Red Cross, Washington DC, USA
[11]International Research Institute for Climate and Society, Columbia University, New York, USA
[12]Lawrence Berkeley National Laboratory, Berkeley, California USA
[13]Department of Geosciences, Princeton University, Princeton, 08544, USA
[14]School of Geography and the Environment, University of Oxford, UK
[15]Department of Earth and Atmospheric Sciences, Cornell University, USA
[16]Climate and Global Dynamics Laboratory, National Center for Atmospheric Research, USA
[17]Canadian Centre for Climate Modelling and Analysis, Environment and Climate Change Canada, Victoria, BC, Canada
[18]Deutscher Wetterdienst, Regionales Klimabüro Potsdam, Potsdam, Germany
[19]Bodeker Scientific, Alexandra, New Zealand
[20]The High Meadows Environmental Institute, Princeton University, Princeton, 08544, USA
[21]Department of Earth, Ocean, and Atmospheric Sciences, The University of British Columbia, Vancouver, Canada

Correspondence: Sjoukje Philip (sjoukje.philip@knmi.nl); Sarah Kew (sarah.kew@knmi.nl)

Abstract. Towards the end of June 2021, temperature records were broken by several degrees Celsius in several cities in the Pacific northwest areas of the U.S. and Canada, leading to spikes in sudden deaths, and sharp increases in hospital visits for heat-related illnesses and emergency calls. Here we present a multi-model, multi-method attribution analysis to investigate to what extent human-induced climate change has influenced the probability and intensity of extreme heatwaves in this region. Based on observations and modeling, the occurrence of a heatwave with maximum daily temperatures (TXx) as observed in the area 45 °N–52 °N, 119 °W–123 °W, was found to be virtually impossible without human-caused climate change. The

https://doi.org/10.5194/esd-2021-90
Preprint. Discussion started: 12 November 2021


Earth System Dynamics Discussions
Open Access
EGU

observed temperatures were so extreme that they lie far outside the range of historically observed temperatures. This makes it hard to quantify with confidence how rare the event was. In the most realistic statistical analysis, which uses the assumption that the heatwave was a very low probability event that was not caused by new nonlinearities, the event is estimated to be about a 1 in 1000 year event in today's climate. With this assumption and combining the results from the analysis of climate models and weather observations, an event, defined as daily maximum temperatures (TXx) in the heatwave region, as rare as 1 in a 1000 years would have been at least 150 times rarer without human-induced climate change. Also, this heatwave was about 2°C hotter than a 1 in 1000-year heatwave that at the beginning of the industrial revolution would have been (when global mean temperatures were 1.2°C cooler than today). Looking into the future, in a world with 2°C of global warming (0.8°C warmer than today), a 1000-year event would be another degree hotter. It would occur roughly every 5 to 10 years in such global warming conditions.

Our results provide a strong warning: our rapidly warming climate is bringing us into uncharted territory with significant consequences for health, well-being, and livelihoods. Adaptation and mitigation are urgently needed to prepare societies for a very different future.

1 Introduction

During the last days of June 2021, Pacific northwest areas of the U.S. and Canada experienced temperatures never previously observed, with records broken in multiple cities by several degrees Celsius. Temperatures far above 40 °C (104 °F) occurred on Sunday 27 to Tuesday 29 June (Figs 1a,b for Monday) in the Pacific northwest areas of the U.S. and western Provinces of Canada, with the maximum warmth moving from the western to the eastern part of the domain from Monday to Tuesday. The anomalies relative to normal maximum temperatures for the time of year reached 16°C to 20 °C (Figs 1c,d). It is noteworthy that these record temperatures occurred one whole month before the climatologically warmest part of the year (end of July, early August), making them particularly exceptional. Even compared to the maximum temperatures in other years independent of the considered month, the recent event exceeds those temperatures by about 5 °C (Figure 2). Records were shattered in a very large area, including setting a new all-time Canadian temperature record in the village of Lytton, at which a temperature of 49.6 °C was measured on June 29 and where wildfires spread on the following day.

Given that the observed temperatures were so far outside historical experiences and in a region with only about 50% household air conditioning penetration, we expect large impacts on health. The excess deaths numbers will be finalized in the coming months. There were 815 deaths in British Columbia, Canada, of which about 70% were heat-related excess deaths.[1] There were nearly 450 extra deaths in Washington and nearly 160 in Oregon.[2]

The present report aims to investigate the role of human-induced climate change in contributing to the likelihood and intensity of this extreme heatwave, following an established approach to multi-model multi-method extreme event attribution (Philip et al., 2020; van Oldenborgh et al., 2021). We focus the analysis on the maximum temperatures in the region where most peo-

[1] https://www.cbc.ca/news/canada/british-columbia/bc-heat-dome-sudden-deaths-570-1.6122316
[2] https://www.nytimes.com/interactive/2021/08/11/climate/deaths-pacific-northwest-heat-wave.html

https://doi.org/10.5194/esd-2021-90
Preprint. Discussion started: 12 November 2021

Earth System Dynamics
Discussions
Open Access
EGU

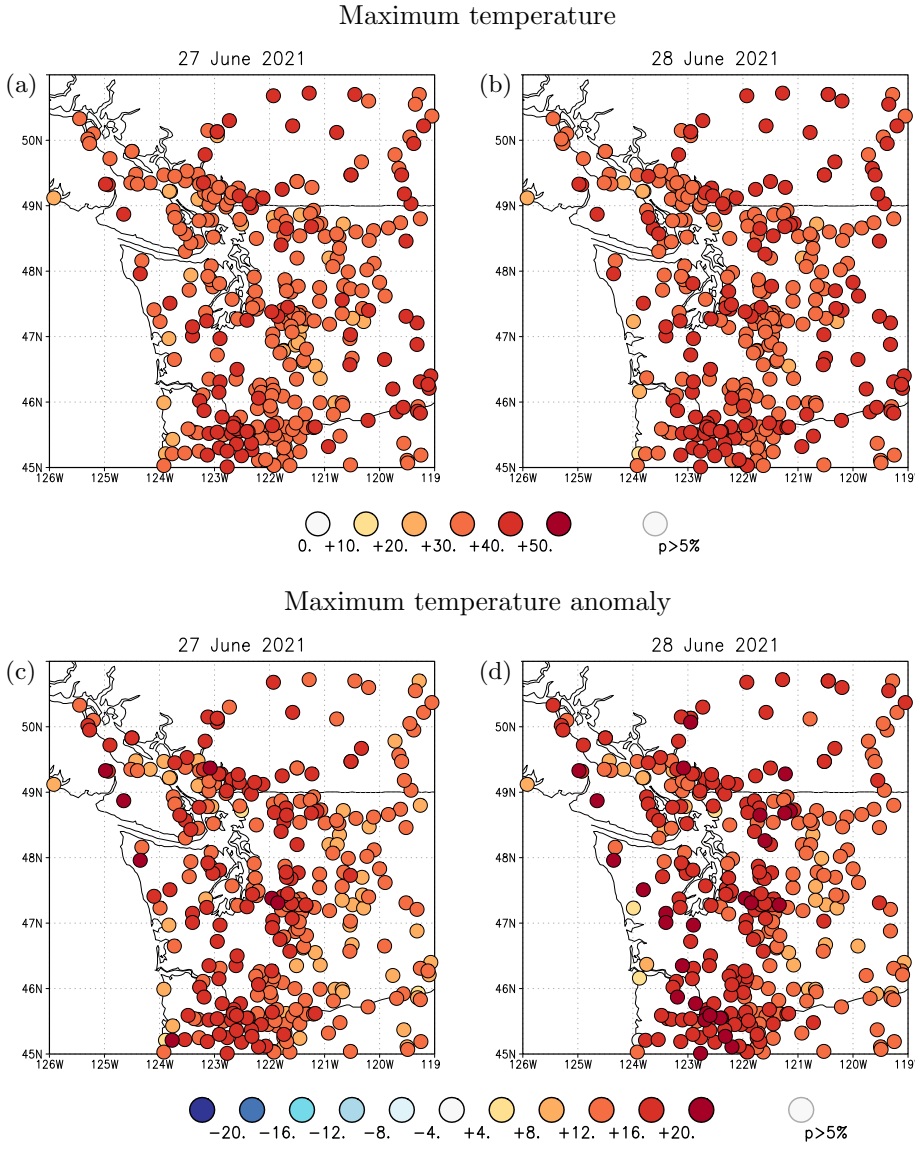

Figure 1. a) observed temperatures on 27 June 2021, b) 28 June 2021, c,d) same for anomalies relative to the whole station records. Source: GHCN-D

ple were affected by the heat (45 °N–52 °N, 119 °W–123 °W) including the cities of Seattle, Portland, and Vancouver. While the extreme heat was an important driver of the observed impacts, it is important to note that these impacts strongly depend on exposure,vulnerability, and other climatological variables beyond temperature. In addition to the attribution of the extreme temperatures we qualitatively assess whether meteorological drivers and antecedent conditions played an important role in the observed extreme temperatures in Section 7.

https://doi.org/10.5194/esd-2021-90
Preprint. Discussion started: 12 November 2021

Earth System Dynamics
Discussions
Open Access
EGU

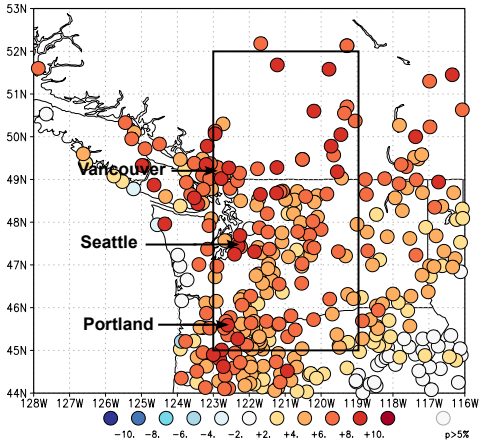

Figure 2. Anomalies of 2021 highest daily maximum temperature (TXx) relative to the whole time series of each station. The black box indicates the study region. Source: GHCN-D

1.1 Event definition

Daily maximum temperatures were the headline figure in the large number of media reports describing the heatwave and the impacts associated with the event. Furthermore, daily maximum temperature was the primary extreme characteristic of the event. We therefore define the event based on the annual maximum of daily maximum temperature, TXx. There is some evidence that longer time scales, e.g. 3-day average, better describe the health impacts (e.g., D'Ippoliti et al., 2010). However, TXx is a standard heat impact index and thus the results can easily be compared to other studies. High minimum temperatures also have strong impacts on human health. However, here we intentionally focus on one event definition to keep this analysis succinct and its results easy to communicate, choosing TXx, which not only characterises the extreme character of the event but is also readily available in climate models allowing us to use a large range of different models. As the spatial scale of the event we consider the area 45°N–52°N, 119°W–123°W. This covers the more populated region around Portland, Seattle and Vancouver that were impacted heavily by the heat (with a total population of over 9.4 million in their combined metropolitan areas), but excludes the rainforest to the west and arid areas to the east. Note that this spatial event definition is based on the expected and reported human impacts rather than on the meteorological extremity. Besides this main definition we also analysed the observations for three stations in Portland, Seattle and Vancouver with long homogeneous time series.

1.2 Previous trends in heatwaves

Figure 3 shows the observed trends in TXx in the GHCN-D dataset over 1900–2019. The stations were selected on the basis of a long time series, at least 50 years of data, and being at least 2°apart. The trend is defined as the regression on the global mean temperature, so the numbers represent how much slower or faster than the global mean the temperature has changed.

https://doi.org/10.5194/esd-2021-90
Preprint. Discussion started: 12 November 2021

Earth System Dynamics
Discussions
Open Access
EGU

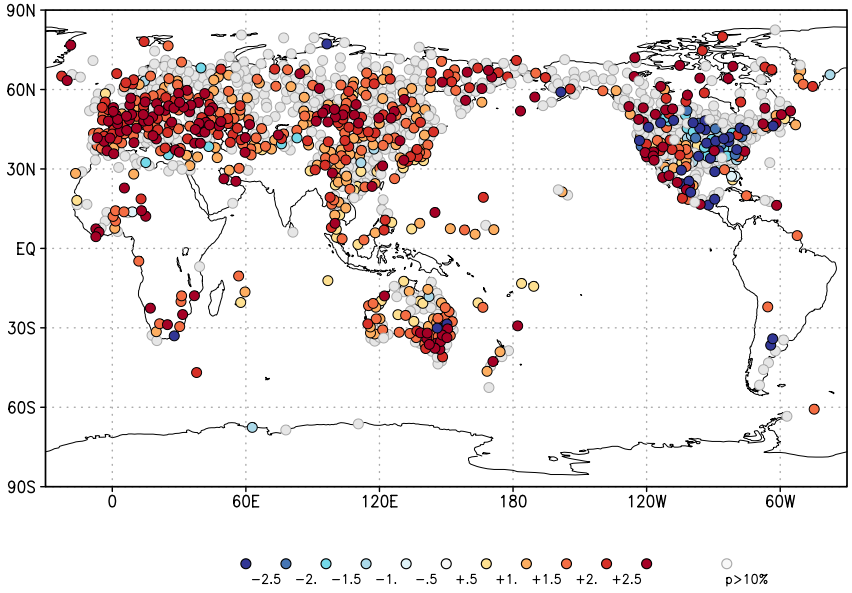

Figure 3. Trends in the highest daily maximum temperature of the year in the GHCN-D station data. Stations are selected to have at least 50 years of data and to be at least 2°apart. The local trends are defined by their regression on the global mean temperature, and shown in units of multiples of the global mean temperature rise. Source: GHCN-D

Individual stations with different trends than nearby stations usually have inhomogeneities in the observational method or local environment. The negative trends in eastern North America and parts of California are well-understood to be the result of land use changes, irrigation and changes in agricultural practice (Donat et al., 2016, 2017; Thiery et al., 2017; Cowan et al., 2020). The large trends in heatwaves in Europe are not yet fully understood or adequately represented in climate models (Vautard et al., 2020). The Pacific Northwest showed trends of about two times the global temperature trend up to 2019.

2 Data and methods

2.1 Observational data

The dataset used to represent the heatwave is the ERA5 reanalysis (Hersbach et al., 2019) from the ECMWF at 0.25°resolution. A very rapid analysis performed directly after the heatwave and published on https://www.worldweatherattribution.org/western-north-american-extreme-heat-virtually-impossible-without-human-caused-climate-change/ used ERA5 extended by the ECMWF operational analysis and the ECMWF forecast. There is only a very minor difference in the heatwave amplitude between the two analyses and this makes no difference to the rounded return period used in this study and the analysis results are therefore not affected.

https://doi.org/10.5194/esd-2021-90
Preprint. Discussion started: 12 November 2021


Earth System Dynamics Discussions
Open Access
EGU

Temperature observations were collected to directly assess the probability ratios and return periods associated with the event for the three major cities in the study area; Portland, Seattle, and Vancouver. Observing sites were chosen that had long homogenized historical records and were representative of the severity of the event by avoiding exposure to nearby large water bodies. Sites were also chosen to be representative of the populous areas of each city to better illuminate impact on inhabitants.

For Portland, the Portland International Airport National Weather Service station was used, which has continuous observations over 1938–2021. The airport is located close to the city centre, adjacent to the Columbia River. The river's influence is thought to be small and the water temperature is warm by June. For Seattle, Seattle-Tacoma International Airport was chosen, which has almost continuous observations 1948–2021, among the longest records in the Seattle area. This location is further inland and lacks the influence of Lake Washington that downtown Seattle has. Two long records exist adjacent to downtown Vancouver, but they are both very exposed to the Georgia Strait that influenced observations due to local onshore flow during the peak of the event. A record was chosen further inland at New Westminster. The observations start in 1875 but here are data gaps 1882–1893, 1928, 1980–1993.

The data for Portland International Airport and Seattle-Tacoma International Airport were gathered from the Global Historical Climatology Network Daily (GHCND; Menne et al., 2012) while data for New Westminster were gathered from the Adjusted Homogenized Canadian Climate Dataset (AHCCD) for daily temperature (Vincent et al., 2020). This station's record is a composite of data from three locations in two nearby cities with location changes in 1966 and 1980. From 1874 to 1966, the station operated at an elevation of 118 m near the centre of New Westminster. In 1966, the station was moved roughly 2 km to the east and to an elevation of 18 m. The portion of the homogenized record from 1980 onward is from Pitt Meadows, BC located roughly 14 km east of the previous location and at an elevation of 5 m. Using a composite station is non-ideal given the potential influence of local micro-climate effects and the increasing distance from the cooling effects of The Strait of Georgia. Those effects may increase the uncertainty of our analysis, but given the magnitude of the signal and the consistency of results among the datasets presented here (and analysis of other temperature records in BC, not shown), we accept these issues. The AHCCD dataset is updated annually and ends in 2020. Data for 2021 were appended from unhomogenized recent records from Environment and Climate Change Canada. Overlapping data for 2020 were compared between the two sources and found to be identical except several duplicate/missing observations which would not cause error in the present analysis because the records are complete for June, 2021.

As a measure of anthropogenic climate change we use the global mean surface temperature (GMST), where GMST is taken from the National Aeronautics and Space Administration (NASA) Goddard Institute for Space Science (GISS) surface temperature analysis (Hansen et al., 2010; Lenssen et al., 2019, GISTEMP,). We apply a 4-yr running mean low-pass filter to suppress the influence of ENSO and winter variability at high northern latitudes as these are unforced variations.

2.2 Model and experiment descriptions

Model simulations from the 6th Coupled Model Intercomparison Project (CMIP6; Eyring et al., 2016) are assessed. We combine the historical simulations (1850 to 2015) with the Shared Socioeconomic Pathway (SSP) projections (O'Neill et al., 2016) for the years 2016 to 2100. Here, we only use data from SSP5-8.5, although the pathways are very similar to each other over

https://doi.org/10.5194/esd-2021-90
Preprint. Discussion started: 12 November 2021


Earth System Dynamics Discussions

the period 2015–2021. Models are excluded if they do not provide the relevant variables, do not run from 1850 to 2100, or include duplicate time steps or missing time steps. All available ensemble members are used. A total of 18 models (88 ensemble members), which fulfill these criteria and passed the validation tests (Section 4), are used.

In addition to the CMIP6 simulations, the ensemble of extended historical simulations from the IPSL-CM6A-LR model is used (see Boucher et al., 2020, for a description of the model). It is composed of 32 members, following the CMIP6 protocol (Eyring et al., 2016) over the historical period (1850-2014) and extended until 2029 using all forcings from the SSP2-4.5 scenario, except for the ozone concentration which has been kept constant at its 2014 climatology (as it was not available at the time of performing the extensions). This ensemble is used to explore the influence of internal variability.

The GFDL-CM2.5/FLOR (Vecchi et al., 2014) is a fully coupled climate model developed at the Geophysical Fluid Dynamics Laboratory (GFDL). While the ocean and ice components have a horizontal resolution of only 1°, the resolution of the atmosphere and land is about 50 km and might therefore provide a better simulation of certain extreme weather events (Baldwin et al., 2019). The data used in this study cover the period from 1860 to 2100, and include both the historical and RCP4.5 experiments driven by transient radiative forcings from CMIP5 (Taylor et al., 2011).

We also examine five ensemble members of the AMIP experiment (1871-2019) from the GFDL-AM2.5C360 (Yang et al., 2021; Chan et al., 2021), which consists of the atmosphere and land components of the FLOR model but with horizontal resolution doubled to 25 km for a potentially better representation of extreme events.

The project (C20C+) was designed specifically for event attribution studies (Stone et al., 2019). The experimental design uses models of the atmosphere and land with prescribed sea surface temperatures and sea ice concentrations, similar to the AMIP experiment. To quantify the impact, if any, on extreme events, participating models were run following the AMIP protocol. The distributions of TXx in the study area were examined in three C20C+ models, CAM5.1, MIROC5 and HadGEM3-A-N216 and compared to that of the ERA5 reanalysis. Only the Community Atmospheric Model (CAM5.1), run at the default ∼1°resolution, satisfied the requirements of this study in the statistical description of heat extremes. The model is described in Neale et al. (2010). The actual world ensemble consists of 99 simulations of mixed duration all ending in 2018 resulting in a sample size of 4090 years. A counterfactual world ensemble of similar size consists of 89 simulations resulting in a sample size of 3823 years.

2.3 Statistical methods

A full description of the statistical methods is given in (Philip et al., 2020; van Oldenborgh et al., 2021). Here we give a summary.

As discussed in section 1.2, we analyse the annual maximum of daily maximum temperatures (TXx) averaged over 45°N-52°N, 119°W-123°W. Initially, we analyse reanalysis data and station data from sites with long records. Next, we analyse climate model output for the same metric. We follow the steps outlined in the WWA protocol for event attribution. The analysis steps include: (i) trend calculation from observations; (ii) model validation; (iii) multi-method multi-model attribution and (iv) synthesis of the attribution statement.

https://doi.org/10.5194/esd-2021-90
Preprint. Discussion started: 12 November 2021


Earth System Dynamics Discussions

For the event under investigation we calculate the return periods, probability ratio (PR) and change in intensity as a function of GMST. The two climates we compared are defined as the GMST of the event year 2021 and a GMST value representative of the climate of the late nineteenth century, -1.2 °C relative to 2021 (1850-1900, based on the Global Warming Index https://www.globalwarmingindex.org). To statistically model the selected event, we use a GEV distribution that shifts with GMST, i.e., the location parameter has a term proportional to GMST and the scale and shape parameters are assumed constant. Next, results from observations and from the models are synthesized into a consistent attribution statement. For models (except for IPSL-CM6A-LR and CAM5.1), we additionally analyse the PR between a future climate at +2°C above the 1850-1900 reference, which is equivalent to +0.8°C above the current climate of 2021. For this analysis we use model data up to about 2050 or when the model GMST reaches +0.8 °C compared to now.

The CMIP6 data are analysed using the same statistical models as the main method. However, the parameter uncertainty is estimated in a Bayesian setting using a Markov Chain Monte Carlo (MCMC) sampler instead of a bootstrapping approach (see Ciavarella et al., 2021, for details).

3 Observational analysis: return time and trend

Time series of various aspects of the main index are shown in Figure 4: a) the daily Tmax evolution from ERA5 (from 1 May to 31 Aug); and b) annual max of the series. The value for 2021, 39.7 °C, is 5.7 °C above the previous record of 34.0 °C, which is an extremely large increase that gives rise to difficulties in the statistical analysis described in Section 3.1. There are two possible sources of this extreme jump in peak temperatures. The first is that a very low probability event occurred — the statistical equivalent of ”really bad luck”. It could have also occurred in pre-industrial climate but its amplitude would have been aggravated by climate change in the current climate which already includes about 1.2°C of global warming. The second option is that strong nonlinear interactions and feedbacks took place in this event with yet unseen temperatures, relative to previous heatwaves, amplifying the intensity of the extreme, a sign that climate change could exacerbate extreme heatwaves beyond expected temperatures. This second possibility needs further research to be confirmed.

In Figure 5a we show the seasonal cycle of the daily maximum temperature averaged over the index region and in Figure 5b the spatial pattern of the annual maximum of the daily maximum temperature at each grid point. These are also used in the model validation procedure.

3.1 Analysis of station and gridded data

Figure 6a shows our standard extreme value analysis and the challenge of applying it to this event. The distribution of our index including data up to 2020 is described very well by a GEV distribution that has linearly warmed at a rate about twice as fast as the GMST. This is consistent with the general characteristic of global warming that summers over continents warm faster than the global mean. The fit has a negative shape parameter ξ, which implies a finite tail, and hence an upper bound. In this case it is at 35.5$\pm$1.3 °C (2σ uncertainty). However, the observed value in 2021, 39.7 °C, is far above this upper bound. Therefore,

https://doi.org/10.5194/esd-2021-90
Preprint. Discussion started: 12 November 2021

Earth System Dynamics
Discussions
Open Access
EGU

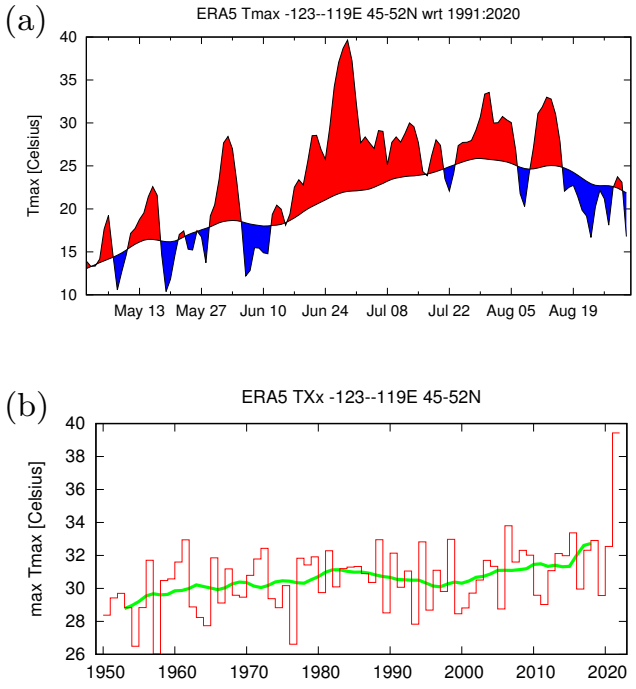

Figure 4. a) Time series for May-Aug 2021 of the maximum daily temperature averaged over the study area based on ERA5, with positive and negative departures from the 1991–2020 climatological mean of daily maximum temperature shaded red and blue, respectively. b) Annual maximum of the index series with a 10-yr running mean (green line). Source: ERA5.

this GEV fit with constant shape and scale parameters that excludes all information about 2021 is not a valid description of the heatwaves in the area.

An alternative to the standard approach of not using any information of the event under study to avoid a selection bias, is to use some of the information from the June 2021 heatwave, namely that it actually happened. Specifically, in the next fit we still assume that the data up to 2020 can be described by a GEV with constant scale and shape parameters, but we reject all GEV models in which the upper bound is below the value observed in 2021. In other words, we enforce fitting to a subset of parameters that are compatible with the 2021 event. The result is shown in Figure 7. While the distribution now includes the 2021 event, the fit to the data up to and including the year 2020 is noticeably worse than when not taking 2021 into account. The return time for the 2021 event under these assumptions still has a lower bound of 10,000 years in the current climate. The fit differs from the previous one mainly in the shape parameter, which is now much less negative (about -0.2 instead of -0.4). This shifts the upper bound to higher values. The fit also gives a somewhat higher trend parameter.

The third possibility is to fit the GEV distribution over all available data, including 2021. This yields a return time of 1,000 years (95% CI >100 yr). This approach implicitly assumes that the 2021 event is drawn from the same population. We could not make this assumption if we had intentionally selected a specific region in order to maximise the extremity of the event — known as selection bias. In intentionally choosing the time series with the largest (rarest) return period for the 2021 event, we

https://doi.org/10.5194/esd-2021-90
Preprint. Discussion started: 12 November 2021

Earth System Dynamics
Discussions
Open Access
EGU

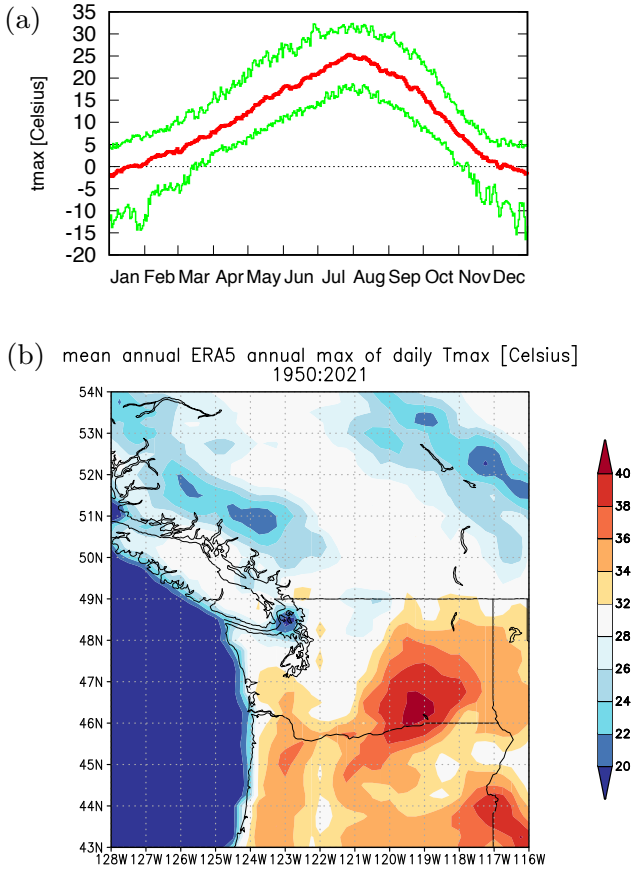

Figure 5. a) Seasonal cycle of Tmax averaged over the land points of 45 °N–52 °N, 119 °N–123 °N, showing the 1950–2021 mean (red) and 2.5% and 97.5% percentiles of the distribution (green). b) Spatial pattern of the 1950–2021 mean of the annual maximum of Tmax at each grid point. Source: ERA5 data.

would in fact be selecting it in preference to others from a larger population of time series and we could not assume the 2021 event to be a representative member of the population for that point alone. This is only partly the case here as we did choose the general region because the heat was exceptional there. However, we also based our exact choice on population density and type of terrain, parameters that are more independent of the heatwave. However, this approach uses all information available and assumes this was just a chance event. We use this third approach thus as the best estimate, although follow-up research will be necessary to investigate the potential reasons of this outstanding event and the consequences on assumptions for these fits (see also the discussion in Section 7). This fit gives a 95% CI of 1.4 K to 1.9 K for the scale parameter σ and -0.5 to 0.0 for the shape parameter ξ. These values are used for the model validation in Section 4.

The detection results, i.e., the comparison of the fit for 2021 and for a pre-industrial climate, show an increase in intensity of TXx of $\Delta T = 3.1$ °C (95% CI: 1.2 to 4.8 °C) and a probability ratio PR of 390 (3.2 to ∞).

https://doi.org/10.5194/esd-2021-90
Preprint. Discussion started: 12 November 2021

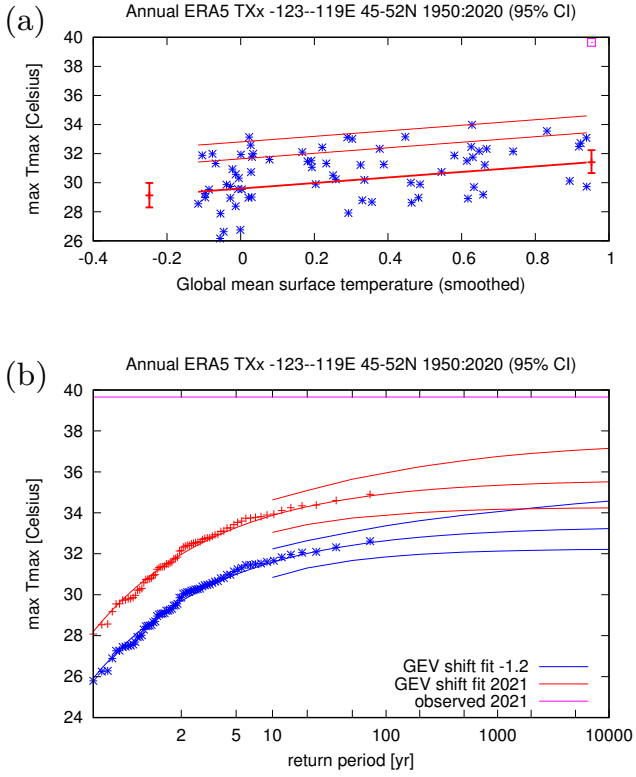

Figure 6. GEV fit with constant scale and shape parameters, and location parameter shifting proportional to GMST of the index series. No information from 2021 is included in the fit. (a): the observed TXx as a function of the smoothed GMST. The thick red line denotes the location parameter, the thin red lines the 6-yr and 40-yr return times. The June 2021 observation is highlighted with the magenta square and is not included in this fit. (b): Return time plots for the climate of 2021 (red) and a climate with GMST 1.2 °C cooler (blue). The red and blue lines indicate the best fit and the 95% confidence intervals, the magenta line shows the observed value. The past observations are shown twice: once shifted up to the current climate and once shifted down to the climate of the late nineteenth century. Source: ERA5, fit: KNMI Climate Explorer.

3.2 Analysis of temperature in Portland, Seattle and Vancouver

For Portland we chose the International Airport station, which is located on the northern edge of the city and has been collecting data since April 1938; the data are in the GHCN-D v2 database. Figure 9 (top panel) shows the annual maxima of the Portland station time series, assuming there will be no higher value during the rest of the year. The record before this year was 41.7 °C in 1965 and 1981, and TXx reached 46.7 °C this year, so the previous record was broken by 5.0 °C.

We fit a GEV distribution to this data, including 2021 (Figure 9, lower panels). It gives a return time of 700 yr for the 2021 event with a lower bound of 70 yr. For the PR we can only give a lower bound of 6, since the best estimate is infinite. This corresponds to an increase in temperature of 3.4 °C with a large uncertainty of 0.3 to 5.3 °C. The large uncertainties are due to the somewhat shorter time series and large variability at this station.

https://doi.org/10.5194/esd-2021-90
Preprint. Discussion started: 12 November 2021

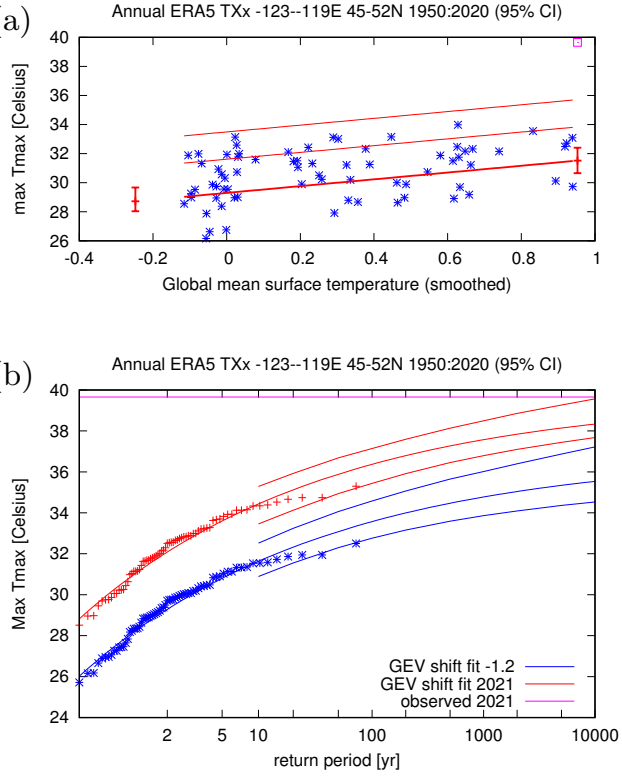

Figure 7. As Figure 6 but demanding the 2021 event is possible in the fitted GEV function, i.e., the upper bound is higher than the value observed in 2021.

In Seattle, the only station with a sufficiently long time series that includes 2021 is Seattle-Tacoma International Airport. It is located ∼15 km south of the city but has similar terrain, without the proximity to water of the city itself. The previous record was 39.4 °C in 2009, and this year it reached 42.2 °C. This is still a large increase of 2.8 °C over the previous record. The event was also not quite as improbable, with a return time of 300 yr (lower bound 40 yr) in the current climate (Figure 10). The PR is again infinite with a lower bound of 7, and the increase in temperature from a late nineteenth century climate is 3.8 °C (0.7 °C to 5.7 °C).

In the Vancouver area the most representative station with the least missing data is New Westminster. It has data from 1875 to 2021 with a few gaps. The previous record was 37.6 °C in 2009, and in 2021 a temperature of 41.4 °C was observed, 4.0 °C warmer. A GEV fit including 2021 gives a return time of 1000 yr with a lower bound of 70 yr (Figure 11). The PR is infinite with a lower bound of 170, and the temperature increased by 3.4 °C (1.9 °C to 5.5 °C).

https://doi.org/10.5194/esd-2021-90
Preprint. Discussion started: 12 November 2021

Earth System Dynamics
Discussions
Open Access
EGU

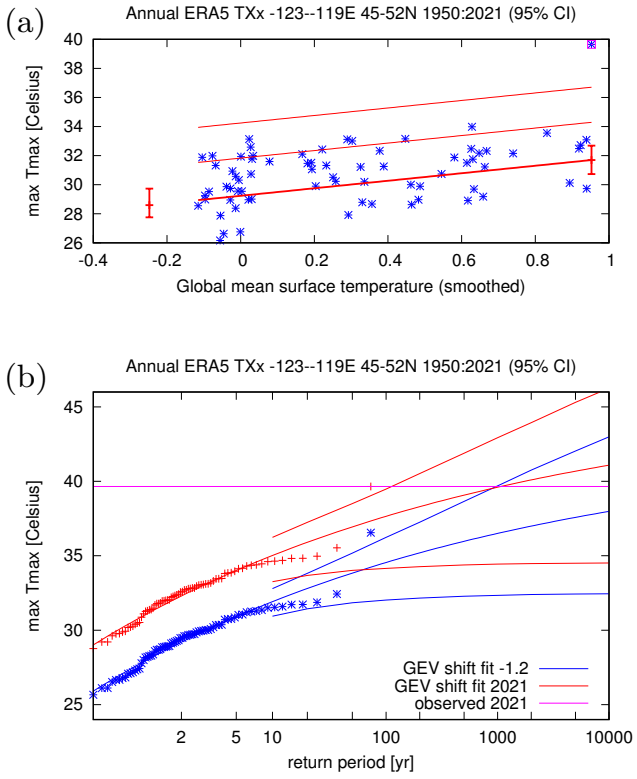

Figure 8. As for Figure 6 but including data from the 2021 heatwave into the fit.

4 Model evaluation

In this section we show the results of the model validation. The validation criteria assess the similarity between the modelled and observed seasonal cycle, the spatial pattern of the climatology, and the scale and shape parameters of the GEV distribution. The assessment results in a label "good", "reasonable" or "bad", according to the criteria defined in Ciavarella et al. (2021). In this study, we use models that are labelled "good" or "reasonable". However, if five or more models are classified as "good" within a particular framing such as the CMIP6 models, then we do not include all of the "reasonable" models but only those that pass the specific test on fit parameters as "good". Table 1 shows the model validation results. The full table including the models that did not pass the validation tests is given in Table 3. 21 models and a combined 224 ensemble members passed the validation test.

5 Multi-method multi-model attribution

This section shows probability ratios and change in intensity ΔT for models that pass the validation tests and also includes the values calculated from the fits to observations (Table 2). Results are given both for changes in current climate (1.2°C) compared

https://doi.org/10.5194/esd-2021-90
Preprint. Discussion started: 12 November 2021

Earth System Dynamics Discussions
Open Access
EGU

Table 1. Validation results for models that pass the validation tests on seasonal cycle, spatial pattern and fitted GEV scale parameter and shape parameter (sigma). Observations in blue, models in black.

Model / Observations (number of members)	**Seasonal cycle**	**Spatial pattern**	**Sigma**	**Shape parameter**	**Conclusion**
ERA5			1.70 (1.40 ... 1.90)	-0.200 (-0.500 ... 0.00)	
GFDL-CM2.5/FLOR historical-rcp45 (5)	good	good	2.01 (1.84 ... 2.17)	-0.201 (-0.272 ... -0.144)	reasonable, include as different experiment than most other models
ACCESS-CM2 historical-ssp585 (2)	good	good	1.86 (1.71 ... 2.02)	-0.200 (-0.260 ... -0.120)	good
AWI-CM-1-1-MR historical-ssp585 (1)	good	good	1.50 (1.35 ... 1.69)	-0.200 (-0.280 ... -0.110)	good
CNRM-CM6-1 historical-ssp585 (1)	good	good	1.54 (1.39 ... 1.72)	-0.210 (-0.290 ... -0.100)	good
CNRM-CM6-1-HR historical-ssp585 (1)	good	good	1.48 (1.33 ... 1.66)	-0.190 (-0.270 ... -0.100)	good
CNRM-ESM2-1 historical-ssp585 (1)	good	good	1.71 (1.54 ... 1.92)	-0.180 (-0.250 ... -0.0900)	good
CanESM5 historical-ssp585 (50)	good	reasonable	1.79 (1.76 ... 1.82)	-0.180 (-0.190 ... -0.170)	reasonable, include because statistical parameters good
EC-Earth3 historical-ssp585 (3)	good	good	1.87 (1.76 ... 2.00)	-0.220 (-0.270 ... -0.170)	good
FGOALS-g3 historical-ssp585 (3)	good	reasonable	1.80 (1.69 ... 1.92)	-0.180 (-0.210 ... -0.140)	reasonable, include because statistical parameters good
GFDL-CM4 historical-ssp585 (1)	good	good	1.43 (1.29 ... 1.62)	-0.210 (-0.300 ... -0.110)	good
INM-CM4-8 historical-ssp585 (1)	good	good	1.63 (1.46 ... 1.83)	-0.210 (-0.300 ... -0.110)	good
INM-CM5-0 historical-ssp585 (1)	good	good	1.80 (1.63 ... 2.03)	-0.240 (-0.310 ... -0.140)	good
IPSL-CM6A-LR historical-ssp585 (6)	good	reasonable	1.79 (1.71 ... 1.88)	-0.220 (-0.250 ... -0.180)	reasonable, include because statistical parameters good
MIROC-ES2L historical-ssp585 (1)	reasonable, peaks early	reasonable	1.46 (1.31 ... 1.65)	-0.190 (-0.300 ... -0.0900)	reasonable, include because statistical parameters good
MPI-ESM1-2-HR historical-ssp585 (2)	good	good	1.49 (1.39 ... 1.62)	-0.250 (-0.310 ... -0.190)	good
MPI-ESM1-2-LR historical-ssp585 (10)	good	good	1.63 (1.58 ... 1.69)	-0.260 (-0.280 ... -0.230)	good
MRI-ESM2-0 historical-ssp585 (2)	reasonable, peak too flat	good	1.41 (1.30 ... 1.53)	-0.280 (-0.340 ... -0.220)	reasonable, include because statistical parameters good
NESM3 historical-ssp585 (1)	good	good	1.48 (1.34 ... 1.67)	-0.290 (-0.370 ... -0.200)	good
NorESM2-MM historical-ssp585 (1)	good	good	1.90 (1.70 ... 2.12)	-0.250 (-0.350 ... -0.140)	in between reasonable and good, include
IPSL-CM6A-LR historical-ssp245 (32)	good, from CMIP6	reasonable, from CMIP6	1.69 (1.64 ... 1.75)	-0.220 (-0.250 ... -0.200)	reasonable, observed GMST used, include
CAM5-1-1degree C20C historical (99)	NA	NA	1.70 (1.68 ... 1.72)	-0.176 (-0.172 ... -0.180)	good, values used with warming level 1.7

https://doi.org/10.5194/esd-2021-90
Preprint. Discussion started: 12 November 2021

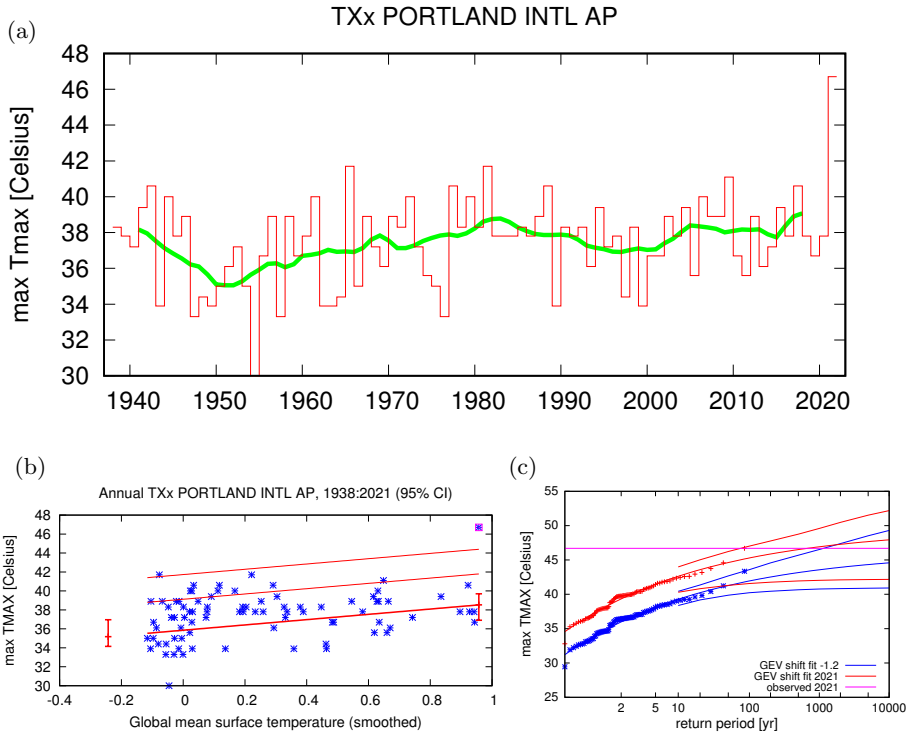

Figure 9. (a) time series of observed highest daily maximum temperature of the year at Portland International Airport. (b,c): as Figure 8 but for the station data at Portland International Airport. Source: data GHCN-D, fit: KNMI Climate Explorer.

to the past (pre-industrial conditions) and, when available, for a climate at +2°C of global warming above pre-industrial climate compared with current climate. The results are visualized in Section 6.

6 Hazard synthesis

We calculate the probability ratio as well as the change in magnitude of the event in the observations and the models. We synthesise the models with the observations to give an overarching attribution statement (please see e.g. Kew et al. (2021) for details on the synthesis technique including how weighting is calculated for observations and for models). Observations and models are combined into a single result in two ways. Firstly, we neglect common model uncertainties beyond the averaged model spread that is depicted by the bright red bar, and compute the weighted average of models and observations: this is indicated by the magenta bar, see Figure 12. The weighting applied is the inverse square of the uncertainty (the width of the bright bars). As, due to common model uncertainties, model uncertainty can be larger than the model spread, secondly, we also show the more conservative estimate of an unweighted average of observations and models, indicated by the white box accompanying the magenta bar in the synthesis figures.

https://doi.org/10.5194/esd-2021-90
Preprint. Discussion started: 12 November 2021

Earth System Dynamics Discussions
Open Access
EGU

Table 2. Analysis results showing the model threshold for a 1-in-1000 year event in the current climate, and the probability ratios and intensity changes for the present climate with respect to the past (labelled "past") and for the +2°C GMST future climate with respect to the present (labelled "future").

Model / Observations (number of members)	**Threshold**	**Probability ratio PR - past [-]**	**Change in intensity ΔT - past [°C]**	**Probability ratio PR - future [-]**	**Change in intensity ΔT - future [°C]**
ERA5	39.7 °C	3.5e+2 (3.2 ... ∞)	3.1 (1.1 ... 4.7)		
GFDL-CM2.5/FLOR historical-rcp45 (5)	34 °C	6.5e+2 (16 ... ∞)	1.6 (1.2 ... 2.1)	4.6 (3.4 ... 12)	1.2 (1.0 ... 1.3)
ACCESS-CM2 historical-ssp585 (2)	35 °C	25 (2.3 ... ∞)	1.1 (0.41 ... 1.9)	45 (4.5 ... ∞)	1.2 (0.96 ... 1.4)
AWI-CM-1-1-MR historical-ssp585 (1)	36 °C	1.1e+4 (6.6 ... ∞)	1.6 (0.84 ... 2.3)	2.8e+2 (5.5 ... ∞)	1.3 (1.1 ... 1.6)
CNRM-CM6-1 historical-ssp585 (1)	34 °C	1.9 (0.0 ... ∞)	0.22 (-0.51 ... 0.95)	69 (3.4 ... ∞)	1.1 (0.76 ... 1.3)
CNRM-CM6-1-HR historical-ssp585 (1)	35 °C	5.2e+2 (5.4 ... ∞)	1.5 (0.73 ... 2.2)	56 (4.1 ... ∞)	1.3 (1.0 ... 1.5)
CNRM-ESM2-1 historical-ssp585 (1)	38 °C	1.5e+2 (3.6 ... ∞)	1.6 (0.68 ... 2.6)	15 (2.8 ... ∞)	0.97 (0.64 ... 1.3)
CanESM5 historical-ssp585 (50)	38 °C	1.6e+3 (2.6e+2 ... 6.7e+4)	2.0 (1.9 ... 2.1)	62 (32 ... 1.5e+2)	1.5 (1.4 ... 1.5)
EC-Earth3 historical-ssp585 (3)	38 °C	3.2e+2 (8.2 ... ∞)	1.3 (0.88 ... 1.7)	20 (5.2 ... 5.8e+2)	1.2 (1.1 ... 1.4)
FGOALS-g3 historical-ssp585 (3)	41 °C	71 (8.5 ... 2.1e+8)	1.5 (1.0 ... 2.0)	17 (5.2 ... 2.2e+2)	1.1 (0.87 ... 1.3)
GFDL-CM4 historical-ssp585 (1)	31 °C	∞ (14 ... ∞)	2.1 (1.3 ... 3.0)	∞ (16 ... ∞)	1.7 (1.4 ... 1.9)
INM-CM4-8 historical-ssp585 (1)	42 °C	∞ (28 ... ∞)	2.6 (1.7 ... 3.6)	2.7e+3 (6.5 ... ∞)	1.7 (1.4 ... 2.0)
INM-CM5-0 historical-ssp585 (1)	41 °C	∞ (14 ... ∞)	2.2 (0.95 ... 3.3)	∞ (12 ... ∞)	1.6 (1.3 ... 2.0)
IPSL-CM6A-LR historical-ssp585 (6)	34 °C	1.5e+5 (50 ... ∞)	1.7 (1.4 ... 2.0)	2.4e+2 (16 ... ∞)	1.3 (1.1 ... 1.4)
MIROC-ES2L historical-ssp585 (1)	33 °C	75 (1.3 ... ∞)	1.2 (0.040 ... 2.3)	12 (2.2 ... ∞)	0.71 (0.41 ... 1.0)
MPI-ESM1-2-HR historical-ssp585 (2)	34 °C	∞ (27 ... ∞)	1.4 (0.82 ... 1.9)	4.8e+4 (12 ... ∞)	1.2 (0.96 ... 1.4)
MPI-ESM1-2-LR historical-ssp585 (10)	32 °C	∞ (1.1e+11 ... ∞)	1.6 (1.4 ... 1.9)	∞ (1.8e+3 ... ∞)	1.3 (1.2 ... 1.4)
MRI-ESM2-0 historical-ssp585 (2)	32 °C	∞ (1.3e+2 ... ∞)	1.4 (0.86 ... 1.9)	13 (4.9 ... 54)	1.0 (0.84 ... 1.2)
NESM3 historical-ssp585 (1)	30 °C	∞ (1.1e+5 ... ∞)	2.5 (1.9 ... 3.2)	∞ (66 ... ∞)	1.5 (1.3 ... 1.7)
NorESM2-MM historical-ssp585 (1)	41 °C	∞ (11 ... ∞)	2.6 (1.3 ... 3.9)	4.3e+7 (7.0 ... ∞)	1.7 (1.3 ... 2.1)
IPSL-CM6A-LR historical-ssp585 (32)	34 °C	∞ (∞ ... ∞)	2.6 (2.4 ... 2.9)	-	-
CAM5-1-1degree C20C historical (99)	43 °C	2.4e+2 (1.5e+2 ... 3.8e+2)	1.6 (1.5 ... 1.8)	-	-

https://doi.org/10.5194/esd-2021-90
Preprint. Discussion started: 12 November 2021

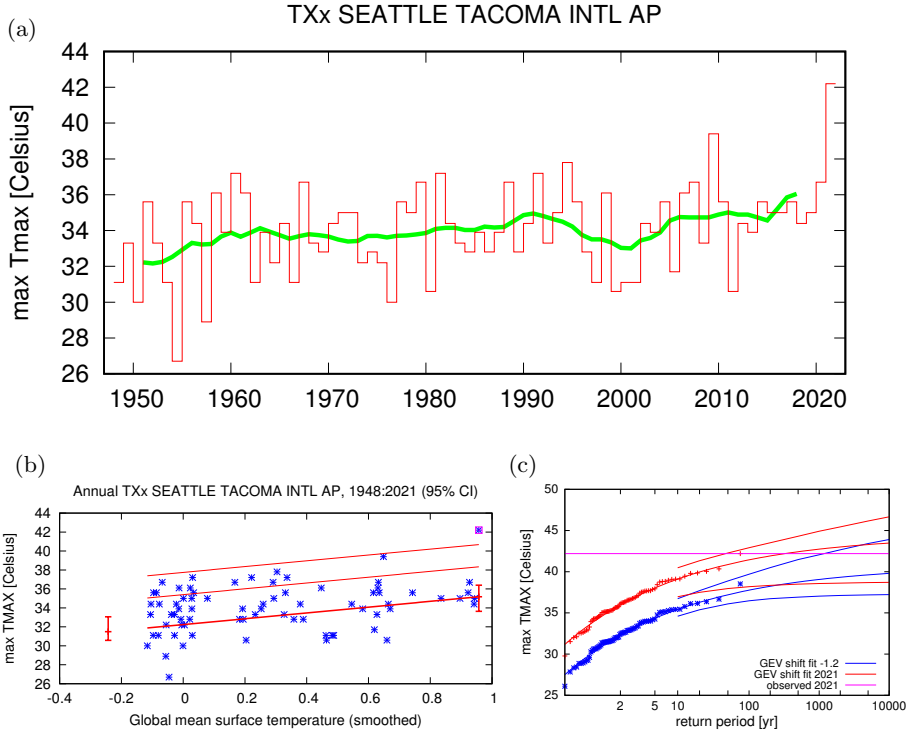

Figure 10. as Figure 9 but for the station data at Seattle-Tacoma International Airport.

Figure 12 shows the synthesis results for the current vs. past climate; the results for the future vs. current climate are presented in Figure 13. Where the results for the probability ratio do not give a finite number we replace them by 10000, to allow all models to be included in the synthesis analysis. This means that the reported synthesized probability ratio gives a more conservative, lower value. For the intensity change we report the weighted synthesis value. For probability ratio we can only give a lower estimate of the range.

Results for current vs past climate, i.e., for 1.2°C of global warming vs pre-industrial conditions (1850-1900), indicate an increase in intensity of about 2.0 °C (1.2 °C to 2.8 °C) and a PR of at least 150. Model results for additional future changes if global warming reaches 2°C indicate a further increase in intensity of about 1.3 °C (0.8 °C to 1.7 °C) and a PR of at least 3, with a best estimate of 175. This means that an event like the current one, that is currently estimated to occur only once every 1000 years, would occur roughly every 5 to 10 years in that future world with 2°C of global warming. Such a 2°C climate could, according to the IPCC AR6 SSP2-4.5 which is the scenario closest to current emission levels, be reached as early as the 2040s (Lee et al., 2021).

https://doi.org/10.5194/esd-2021-90
Preprint. Discussion started: 12 November 2021

Earth System Dynamics
Discussions
Open Access
EGU

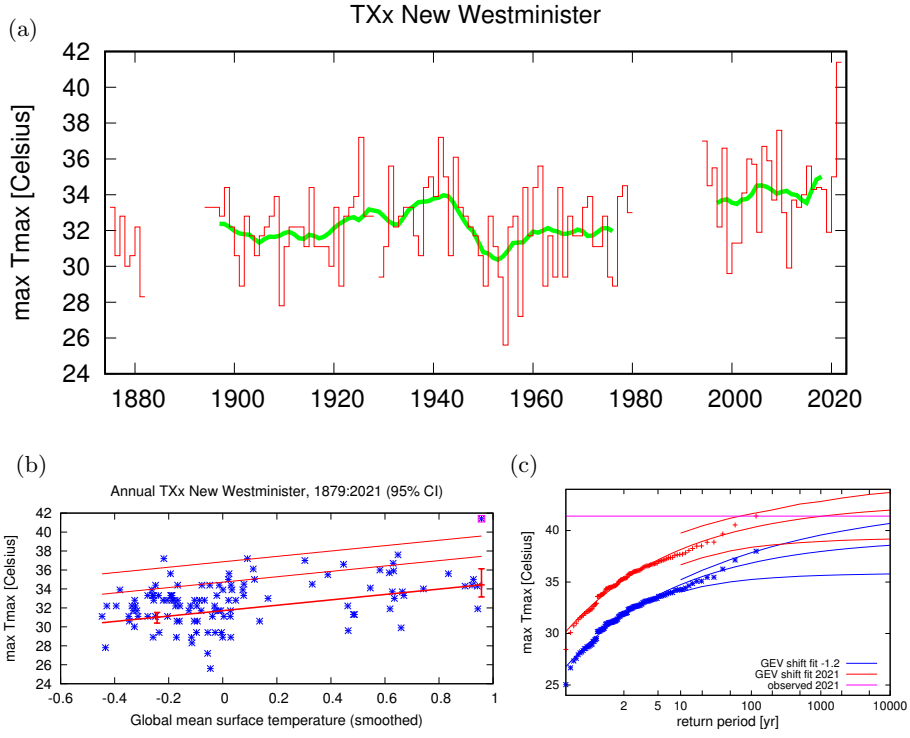

Figure 11. as Figure 9 but for the station data at New Westminster. Source: see text.

7 The broader context of the heatwave

In this discussion section we discuss the probabilities of extreme heatwaves in a broader perspective and the meteorological conditions and other factors that possibly influenced the extremity of this heatwave event.

7.1 Probability of a chance event

In this study our analysis focuses on the Pacific North West heatwave event for the specific area 45°N-52°N, 119°W-123°W. We can give a very rough estimate of the global return time for an event of similar scale, with a sudden jump in TXx with a similar return time. The entire heatwave covers an area of O(1500 km)^2, which is about 1.5% of the land area of the world. Assuming it was just a chance event, we can estimate the return time of a similar heatwave in terms of probability and area covered, as there are about 1/(1.5%) $\sim$ 60 independent areas in which it could have occurred. This implies that the return time of an event as rare as this one or rarer, somewhere over land, is about 60 times smaller than the O(1000 yr) that it occurred at the specific location that it did. This gives a very rough estimate of O(15 yr) with a lower bound of O(1.5 yr) (not shown) to have such a heatwave somewhere on the land of the earth. It is therefore conceivable that it was pure chance that it happened at this location. Further research on this and other exceptional heatwaves is needed to determine whether this estimate is indeed realistic, i.e., whether or not we should reject the assumption that this heatwave occurred by chance at this location.

https://doi.org/10.5194/esd-2021-90
Preprint. Discussion started: 12 November 2021

Earth System Dynamics Discussions
Open Access
EGU

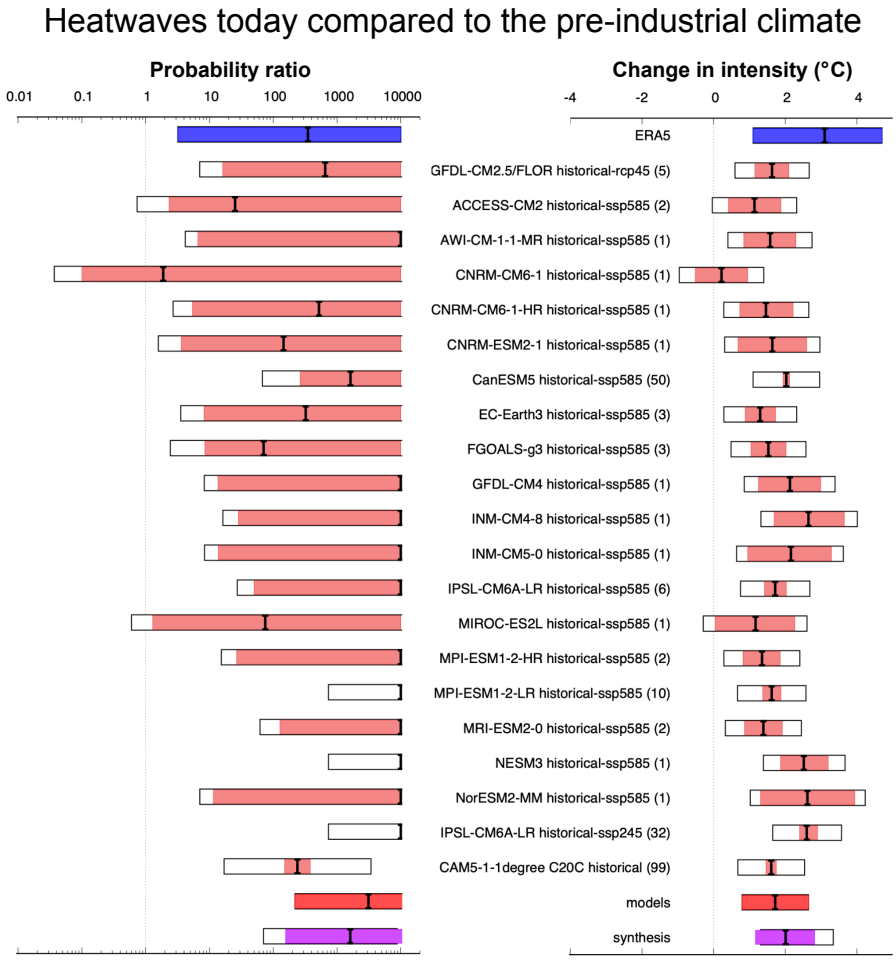

Figure 12. Synthesis of the past climate, showing probability ratios (left) and changes in intensity in °C (right), comparing the 2021 event with a pre-industrial climate.

7.2 Meteorological analysis and dynamics

The evolution of this event can be explained by a confluence of meso- and synoptic-scale dynamical features, potentially including antecedent low soil moisture conditions and anomalously high column specific humidity that are a hallmarks of extreme heat in western North America (Stewart et al., 2017; Bumbaco et al., 2013). At the synoptic scale, an omega-block developed over the study area beginning at roughly 00UTC on June 25th centred at ∼125 °W, 52 °N, which then slowly progressed eastward over subsequent days. This ridge featured a maximal 500 hpa geopotential height of ∼5980 m, which is unprecedented for this area of western North America for the period from 1948 through to June 2021 at least (Figure 14).

Despite being a record, this extreme high pressure system – a feature sometimes called a ”Heat dome” – is not that anomalous given the long-term trend in 500 hPa driven by thermal expansion (Christidis and Stott, 2015). Also, comparing recent

https://doi.org/10.5194/esd-2021-90
Preprint. Discussion started: 12 November 2021

Earth System Dynamics
Discussions
Open Access
EGU

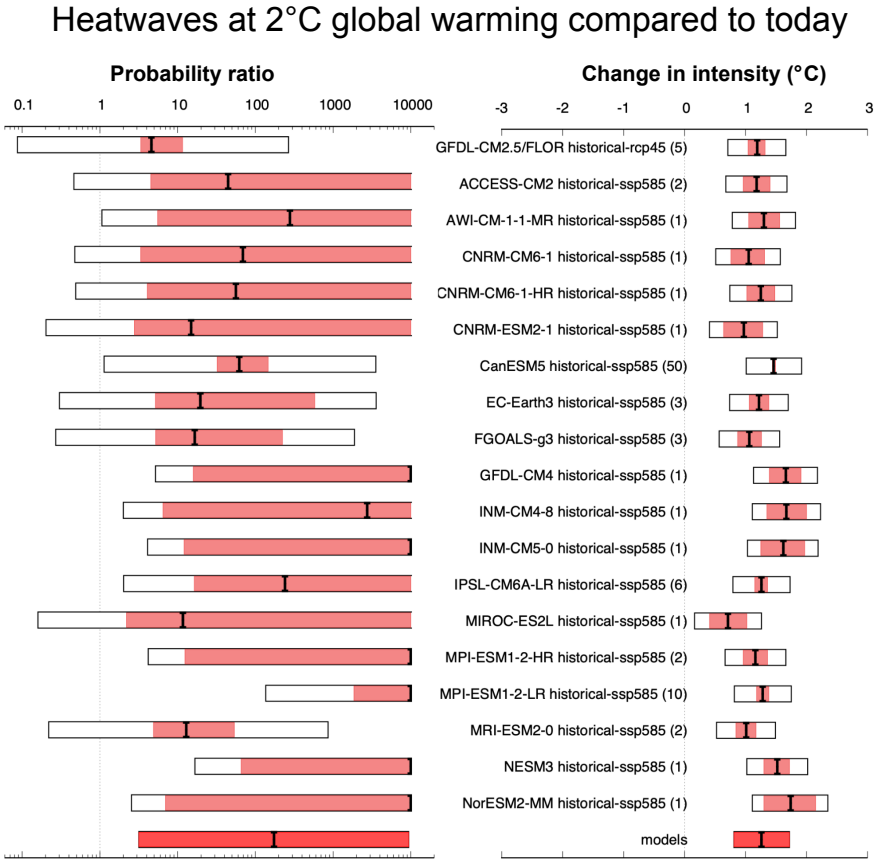

Figure 13. Same as Figure 12 but comparing 2°C of global warming (above pre-industrial) with present-day values.

heatwaves in the Pacific NW to the extreme heatwave in Western Europe in 2019 (Vautard et al., 2020), the geopotential height reached similar anomalies and has a similar long-term trend (Figure 14).

The circulation pattern itself also appears typical for hot summertime temperature: using analogues of 500 hPa and a pattern correlation metric to compare fields, we find that about 1% of June and July circulation patterns, defined as the 500 hPa geopotential height pattern within [160 °W-110 °W; 35 °N-65 °N] in previous years have an anomaly correlation larger than 0.8 with the 28 June pattern. This degree of correlation is typical among days with this type of blocking pattern during the months of June and July. Roughly one third of June and July geopotential height fields have 1% or fewer analogues with an anomaly correlation larger than 0.8. We also find that this fraction does not change when restricting the analogues search within 3 distinct time periods between 1948 and 2020. We conclude that the 28 June circulation is likely not exceptional, while temperatures associated with it were.

At the meso-scale, high solar irradiance during the longest days of the year and strong subsidence increased near-surface air temperatures during the event. As is typical for summer heatwaves in the region (Brewer et al., 2012, 2013), a meso-scale thermal trough developed over western Oregon by 00UTC on the 28th June. This feature migrated northward reaching the

https://doi.org/10.5194/esd-2021-90
Preprint. Discussion started: 12 November 2021

Earth System Dynamics
Discussions
Open Access
EGU

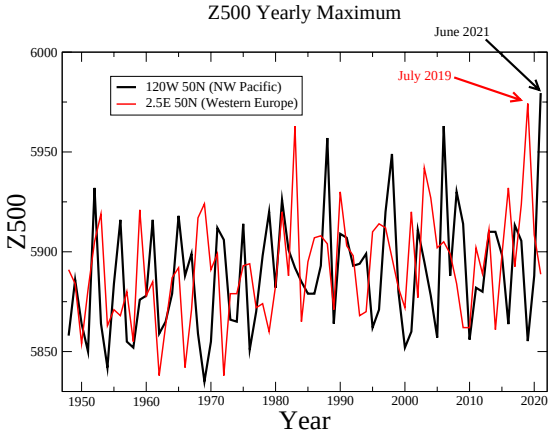

Figure 14. Annual maximum 500 hPa height (m) for two points at the same latitude in two continents. Black: Pacific NW (as above) and red: Western Europe (2.5E; 50N). Data source: NCEP initialized reanalysis.

northern tip of Washington State by 00UTC on the 29th. Further offshore, a small cut-off low travelled southwest to northeast around the synoptic-scale trough that made up the west arm of the omega block. The pressure gradients associated with the thermal trough and the cut-off low promoted moderate E-SE flow in the northern and eastern sectors of the feature and S-SW flow to the south. Near-surface winds with easterly components crossed the Cascade Range of Washington and Oregon and the southern Coast Mountains of British Columbia where they were lighter but sufficient to displace cooler marine air. The difference in elevation on the west and east sides of the mountain ranges contributed to more adiabatic heating than cooling, which helped drive the warmest temperatures observed in the event along the foot of the west slope of these mountains, near or slightly above sea level. These dynamics are illustrated in Figure 15. By 12UTC on the 29th of June 2021, all but the eastern edge of the study area was under the influence of southerly to southwesterly near surface flows that advected marine air and forced marked cooling. Unfortunately, winds associated with this transition intensified a wildfire that quickly consumed the town of Lytton, BC where Canada's nationwide all time high temperature was set just a day before.

There is no scientific consensus whether blocking events are made more severe or persistent because of Arctic amplification or other mechanisms (i.e. Tang et al., 2014; Barnes and Screen, 2015; Vavrus, 2018). We contend that Arctic sea-ice was unlikely to have played a large role in this event largely due to the timing. In early summer, Arctic sea ice remains extensive, but is melting thus keeping near surface temperatures near 0 °C. This causes summer trends in near-surface temperatures over the Arctic ocean to be smaller than for the midlatitudes. During the months prior to the event, the sea ice extent was below the 1981-2010 mean, but was similar to values observed from 2011 to 2020 (Fetterer et al., 2017 (updated daily). Instead, Arctic Amplification in summer is characterized by strong warming over high-latitude land areas (as can clearly be seen in Figure 16) and this warming signal reaches into the upper-troposphere. This enhanced warming is likely related to strong downward trends in early summer snow cover. There is evidence, from observations (Coumou et al., 2015; Chang et al., 2016), climate

https://doi.org/10.5194/esd-2021-90
Preprint. Discussion started: 12 November 2021

Earth System Dynamics
Discussions
Open Access
EGU

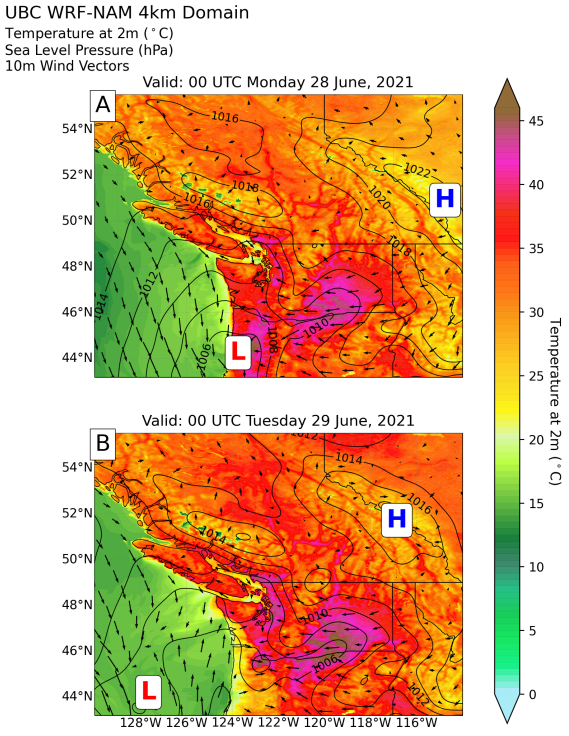

Figure 15. Regional simulation of sea level pressure, 2m air temperature, and 10m wind velocity in the region containing the study area using the Weather Research and Forecasting (WRF Skamarock et al., 2019) model forced by the North American Mesoscale Forecast System (NAM). Panel (A) shows the situation during the peak of the event for the part of the study area south of Portland at 5PM local time. Panel (B) as in (A) but for 5PM local time on the day of peak temperature for Portland, Seattle and Vancouver.

models (Harvey et al., 2020; Lehmann et al., 2014) and paleo-proxies (Routson et al., 2019), that this enhanced warming over high latitudes leads to a weakening of the jet and storm tracks in summer. This weakening could favour more persistent weather conditions (Pfleiderer et al., 2019; Kornhuber and Tamarin-Brodsky, 2021). Regional-scale interactions between loss of snow cover and low soil moisture associated with earlier snowmelt and rapid springtime soil moisture drying, may have had an enhanced warming impact into early summer in the Arctic. At mid-atmospheric levels there is some amplification remaining due to the winter season (Figure 16), but at the jet level (∼250 hPa) the usual increase of the thermal gradient due to tropical upper tropospheric warming is advected North by the Hadley circulation (Haarsma et al., 2013). The final effect on the jet stream is therefore a competition between factors enhancing and decreasing the temperature gradient.

https://doi.org/10.5194/esd-2021-90
Preprint. Discussion started: 12 November 2021

Earth System Dynamics
Discussions
Open Access
EGU

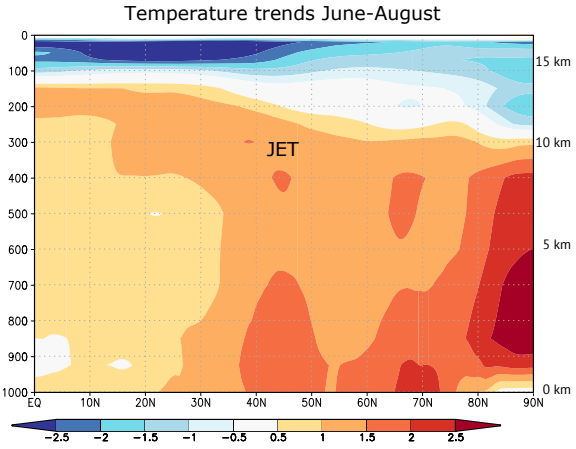

Figure 16. Zonal mean trends in temperature (°C per degree global warming) as function of pressure (hPa) in the ERA5 reanalysis 1979–2019 in the northern hemisphere.

7.3 Drought

An additional feature of the event is the very dry antecedent conditions that may have contributed to observed extreme temperatures through reduced latent cooling from low evapotranspiration rates. Low soil moisture conditions can lead to a strong amplification of temperature during heatwaves, including non-linear effects (Seneviratne et al., 2010; Mueller and Seneviratne, 2012; Hauser et al., 2016; Wehrli et al., 2019). In addition, low spring snow level conditions can also further amplify this feedback (Hall et al., 2008). Integrated Multi-satellitE Retrievals for the Global Precipitation Mission (IMERG) estimates of precipitation during the period from March through June, 2021 indicate anomalously dry conditions from southern BC southward through California (Figure 17). The precipitation anomaly ranges from close to zero over the Puget Sound area including Seattle to values of between -0.6 and -0.8, meaning that only 20-40% of the average amount of precipitation fell in these locations, in Western Oregon. Note that in the northern parts of the area affected by the heatwave, i.e., in the coastal mountains north of Vancouver Island, large positive precipitation anomalies occurred over the months prior to the event.

The available moisture is also influenced by evapotranspiration, which depends strongly on temperature, radiation and available atmospheric moisture. Evaporation was close to normal in the ERA5 reanalysis March–May in this area (not shown), so does not seem to have played a large role in setting the stage for the heatwave.

Satellite-based measurements of surface soil moisture based on microwave remote sensing from the European Space Agency (ESA) Climate Change Initiative (CCI) provided by the Copernicus service suggest that surface soil moisture was below normal in the region since the beginning of April and that the anomalous conditions persisted until June (https://dataviewer.geo.tuwien.ac.at/?state=88bf0c), in agreement with the decreased precipitation and close to normal evapotranspiration in the ERA5 reanalysis.

https://doi.org/10.5194/esd-2021-90
Preprint. Discussion started: 12 November 2021

Earth System Dynamics
Discussions
Open Access
EGU

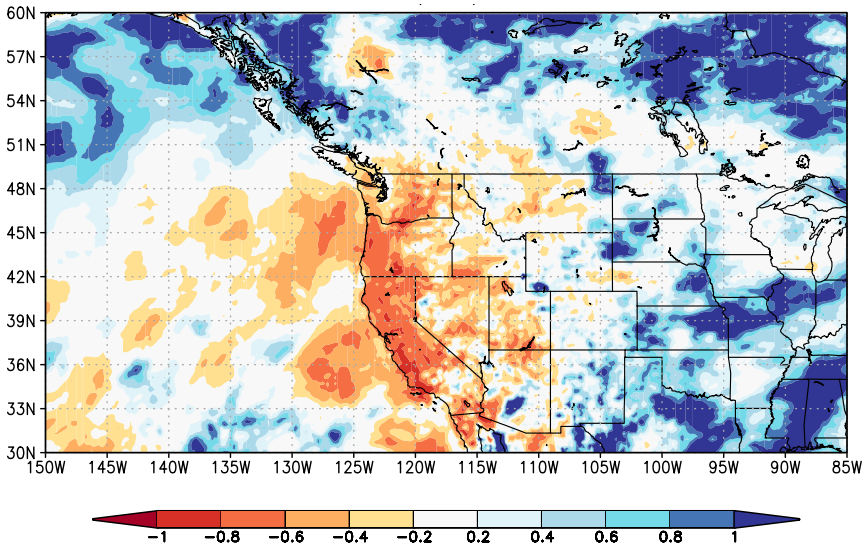

Figure 17. GPM/IMERG satellite estimates of relative precipitation anomalies in March–June 2021 relative to the whole record (2000-2020). The value –1 (dark red) denotes no precipitation, –0.5 (orange) 50% less than normal and zero (light grey) normal precipitation. Fit: KNMI Climate Explorer.

7.4 Influence of modes of natural variability

The El Niño Southern Oscillation is the dominant source of interannual variability in the region through the Pacific North American teleconnection. The influence is typically greatest in late winter and spring and has less clear impacts during summer and fall. Because ENSO was neutral during the preceding months and the impacts on TXx are minimal ($r<0.1$) we conclude that it had no influence on the occurrence of the heatwave.

The Pacific Decadal Oscillation (PDO) can affect some aspects of North American summer weather, although again the connections to heatwaves in this region are very weak. The strongly negative values of the PDO index, as they occurred in May, would slightly favor cooler conditions for this region. PDO thus also is unlikely to have played an important role in the event.

Altogether, external modes of variability appear to have played little to no role in the formation of the event.

8 Vulnerability and exposure

The Pacific Northwest region is not accustomed to very hot temperatures such as those experienced during the June 2021 heatwave. Heatwaves are one of the deadliest natural hazards, resulting in high excess mortality through direct impacts of heat (e.g. heat stroke) and by exacerbating pre-existing medical conditions linked to respiratory and cardiovascular issues (Haines

https://doi.org/10.5194/esd-2021-90
Preprint. Discussion started: 12 November 2021


Earth System Dynamics Discussions Open Access EGU

et al., 2006; Ebi et al., 2021). In addition to more than 1,000 excess heat-related deaths, there was a significant increase in emergency department visits.[3][4] On June 28, 2021 alone, there were 1,038 heat-related emergency department visits in the U.S. Department of Health and Human Services Region that includes Alaska, Idaho. Oregon, and Washington, compared with nine visits on the same date in 2019.[5] The mean daily number of heat-related illness emergency department visits in the region for 25-30 June 2021(424) was 69-times higher than during the same days in 2019 (6). Although this region covers about 4% of the US population, it accounted for about 15% of all heat-related illness emergency department visits nationwide during June.

The June 2021 heatwave also affected critical infrastructure such as roads and rail and caused power outages, agricultural impacts, and forced many businesses and schools to close.[6] [7] Rapid snowmelt in BC caused water levels to rise, leading to evacuation orders north of Vancouver.[8] Furthermore, in some places, wildfires, the risk of which has increased due to climate change in this region (Kirchmeier-Young et al., 2019), started and quickly spread, requiring entire towns to evacuate.[9] The co-occurence of such events may result in compound risks, for example as households are advised to shut windows to keep outdoor wildfire smoke from getting inside, while simultaneously threatened by high indoor temperatures when lacking air conditioning.

Timely warnings were issued throughout the region by the US National Weather Service, Environment and Climate Change Canada, and local governments. British Columbia has a ”Municipal Heat Response Planning” summary review that gathers information on heat response plans throughout the province, including responses such as increasing access to cooling facilities and distribution of drinking water. In long-term strategies, changes to the built environment are emphasized (Lubik et al., 2017). Not all municipalities throughout the Pacific Northwest and BC have formalized heat response plans, and others have limited planning, thought to be due to low heat risk perceptions throughout the area, as well as a lack of local data for risk assessments (Lubik et al., 2017).

The extremely high temperatures that occurred in this heat episode meant that everyone was vulnerable to its effects if exposed for a long enough period of time. Although extreme heat affects everyone, some individuals are more vulnerable, including the elderly, young children, individuals with pre-existing medical conditions, socially isolated individuals, homeless people, individuals without air-conditioning, and (outdoor) workers (Singh et al., 2019). Seattle’s King County contains the third-largest population of homeless people in the U.S, with the numbers increasing during the past decade (Stringfellow and

[3]https://www.nytimes.com/interactive/2021/08/11/climate/deaths-pacific-northwest-heat-wave.html
[4]https://www.cbc.ca/news/canada/british-columbia/bc-heat-dome-sudden-deaths-570-1.6122316
[5]https://www.cdc.gov/mmwr/volumes/70/wr/mm7029e1.htm
[6]https://apnews.com/article/canada-heat-waves-environment-and-nature-cc9d346d495caf2e245fc9ae923adae1
[7]https://www.seattletimes.com/seattle-news/weather/pacific-northwests-record-smashing-heat-wave-primes-wildfire-buckles-roads-health-toll-not-yet-known
[8]https://globalnews.ca/news/7994540/flooding-record-breaking-heat-rapid-snow-melt-bc-video/
[9]https://www.washingtonpost.com/world/2021/07/01/lytton-canada-evacuated-wildfire-heatwave/

https://doi.org/10.5194/esd-2021-90
Preprint. Discussion started: 12 November 2021


Earth System Dynamics Discussions Open Access EGU

Wagle, 2018). Governmental authorities opened cooling centres throughout Seattle, Portland, and Vancouver BC during the June 2021 heatwave. [10] [11] [12] Further, electrolytes, food, and water were distributed to homeless people. [13]

The lack of air conditioning contributes to heat risk. The Pacific Northwest has lower access to air-conditioned homes and buildings compared to other regions in the U.S., with the Seattle metropolitan area being the least air-conditioned metropolitan area of the United States (<50% air conditioning in residential areas) (U.S. Census Bureau). Portland and Vancouver also have low percentages of air-conditioned households, 79% and 39% respectively (BC Hydro; U.S. Census Bureau). An increasing trend in air conditioned homes is occurring in all three cities (ibid.).

9 Conclusions and recommendations

In this study, the influence of human-induced climate change on the intensity and probability of the Pacific Northwest heatwave of 2021 was investigated. We analysed the heat in the area 45 °N–52 °N, 119 °W–123 °W that includes the cities Vancouver, Seattle and Portland. Based on the analysis of annual maximum daily maximum temperatures in weather observations and modeling, we conclude that the occurrence of a heatwave of the intensity experienced in that area would have been virtually impossible without human-caused climate change. Such an event is estimated to be a one in 1000-yr event in the current climate and would have been at least 150 times rarer without human-induced climate change. Also, this heatwave was about 2 °C (1.2 °C to 2.8 °C) hotter due to human induced climate change. Looking into the future to a world with 2 °C of global warming, an event like this, currently estimated to occur only once every 1000 years, would occur roughly every 5 to 10 years.

Adaptation measures need to be much more ambitious and take account of the rising risk of heatwaves around the world. Although this extreme heat event is still rare in today's climate, the analysis above shows that the frequency is increasing with further warming. Deaths from extreme heat can be dramatically reduced with adequate preparedness action – a number of adaptation and risk management priorities emerge. It is crucial that local governments and their emergency management partners establish heat action plans to ensure well coordinated response actions during an extreme heat event - tailored to high-risk groups (Ebi, 2019). Heatwave early warning systems also need to be improved, which includes tailoring messages to inform and motivate vulnerable groups, as well as providing tiered warnings that take into account vulnerable groups may have lower thresholds for risk (Hess and Ebi, 2016). In other words, it is important to start to warn the most vulnerable as temperatures start to rise even though the general population is not yet acutely at risk. In cases where heat action plans and heat early warning systems are already robust, it is important that they are reviewed and updated to capture the implications of rising risks - every five years or less (Hess and Ebi, 2016). Further, heatwave early warning systems should undergo stress tests to evaluate their robustness to temperature extremes beyond recent experience and to identify modifications to ensure continued effectiveness in a changing climate (Ebi et al., 2018).

[10] https://durkan.seattle.gov/2021/06/city-of-seattle-opens-additional-cooling-centers-and-updated-guidance-for-staying-cool-in-extreme-heat%E2%80%AF/

[11] https://www.oregonlive.com/weather/2021/06/portland-cooling-centers-provide-relief-from-heat.html

[12] https://thebcarea.com/2021/06/26/cooling-stations-set-up-around-b-c-for-record-breaking-heat-wave-this-weekend/#comments

[13] https://edition.cnn.com/2021/06/29/weather/northwest-heat-illness-emergency-room/index.html

https://doi.org/10.5194/esd-2021-90
Preprint. Discussion started: 12 November 2021

Earth System Dynamics Discussions Open Access EGU

Data availability. Data are available via the KNMI Climate Explorer (https://climexp.knmi.nl/)

Appendix A: Validation tables

Table A1: As Table 1 but showing all model validation results.

Model / Observations (number of members)	**Seasonal cycle**	**Spatial pattern**	**Sigma**	**Shape parameter**	**Conclusion**
ERA5			1.70 (1.40 ... 1.90)	-0.200 (-0.500 ... 0.00)	
GFDL-CM2.5/FLOR historical-rcp45 (5)	good	good	2.01 (1.84 ... 2.17)	-0.201 (-0.272 ... -0.144)	reasonable, include as different experiment than most other models
ACCESS-CM2 historical-ssp585 (2)	good	good	1.86 (1.71 ... 2.02)	-0.200 (-0.260 ... -0.120)	good
ACCESS-ESM1-5 historical-ssp585 (2)	good	good	2.69 (2.49 ... 2.90)	-0.240 (-0.290 ... -0.190)	bad
AWI-CM-1-1-MR historical-ssp585 (1)	good	good	1.50 (1.35 ... 1.69)	-0.200 (-0.280 ... -0.110)	good
BCC-CSM2-MR historical-ssp585 (1)	good	good	2.22 (2.00 ... 2.49)	-0.230 (-0.310 ... -0.140)	bad
CAMS-CSM1-0 historical-ssp585 (1)	good	good	1.98 (1.79 ... 2.23)	-0.200 (-0.290 ... -0.100)	reasonable, exclude because enough good CMIP5 models
CMCC-CM2-SR5 historical-ssp585 (1)	good	good	1.29 (1.15 ... 1.46)	-0.0800 (-0.160 ... 0.0300)	reasonable, exclude because enough good CMIP5 models
CNRM-CM6-1 historical-ssp585 (1)	good	good	1.54 (1.39 ... 1.72)	-0.210 (-0.290 ... -0.100)	good
CNRM-CM6-1-HR historical-ssp585 (1)	good	good	1.48 (1.33 ... 1.66)	-0.190 (-0.270 ... -0.100)	good
CNRM-ESM2-1 historical-ssp585 (1)	good	good	1.71 (1.54 ... 1.92)	-0.180 (-0.250 ... -0.0900)	good
CanESM5 historical-ssp585 (50)	good	reasonable	1.79 (1.76 ... 1.82)	-0.180 (-0.190 ... -0.170)	reasonable, include because statistical parameters good
EC-Earth3 historical-ssp585 (3)	good	good	1.87 (1.76 ... 2.00)	-0.220 (-0.270 ... -0.170)	good
EC-Earth3-Veg historical-ssp585 (4)	good	good	2.07 (1.95 ... 2.19)	-0.250 (-0.290 ... -0.210)	bad
FGOALS-g3 historical-ssp585 (3)	good	reasonable	1.80 (1.69 ... 1.92)	-0.180 (-0.210 ... -0.140)	reasonable, include because statistical parameters good
GFDL-CM4 historical-ssp585 (1)	good	good	1.43 (1.29 ... 1.62)	-0.210 (-0.300 ... -0.110)	good
GFDL-ESM4 historical-ssp585 (1)	good	good	1.37 (1.23 ... 1.55)	-0.170 (-0.260 ... -0.0700)	reasonable, exclude because enough good CMIP5 models

https://doi.org/10.5194/esd-2021-90
Preprint. Discussion started: 12 November 2021

Earth System Dynamics Discussions Open Access EGU

HadGEM3-GC31-LL historical-ssp585 (4)	good	good	2.00 (1.90 ... 2.12)	-0.210 (-0.250 ... -0.170)	reasonable, exclude because enough good CMIP5 models
HadGEM3-GC31-MM historical-ssp585 (3)	good	good	2.08 (1.96 ... 2.22)	-0.190 (-0.230 ... -0.140)	bad
INM-CM4-8 historical-ssp585 (1)	good	good	1.63 (1.46 ... 1.83)	-0.210 (-0.300 ... -0.110)	good
INM-CM5-0 historical-ssp585 (1)	good	good	1.80 (1.63 ... 2.03)	-0.240 (-0.310 ... -0.140)	good
IPSL-CM6A-LR historical-ssp585 (6)	good	reasonable	1.79 (1.71 ... 1.88)	-0.220 (-0.250 ... -0.180)	reasonable, include because statistical parameters good
KACE-1-0-G historical-ssp585 (3)	good	good	2.27 (2.13 ... 2.41)	-0.241 (-0.282 ... -0.196)	bad
MIROC-ES2L historical-ssp585 (1)	reasonable, peaks about a month early	reasonable	1.46 (1.31 ... 1.65)	-0.190 (-0.300 ... -0.0900)	reasonable, include because statistical parameters good
MIROC6 historical-ssp585 (50)	good	good	1.31 (1.29 ... 1.33)	-0.220 (-0.220 ... -0.210)	bad
MPI-ESM1-2-HR historical-ssp585 (2)	good	good	1.49 (1.39 ... 1.62)	-0.250 (-0.310 ... -0.190)	good
MPI-ESM1-2-LR historical-ssp585 (10)	good	good	1.63 (1.58 ... 1.69)	-0.260 (-0.280 ... -0.230)	good
MRI-ESM2-0 historical-ssp585 (2)	reasonable, peak too flat	good	1.41 (1.30 ... 1.53)	-0.280 (-0.340 ... -0.220)	reasonable, include because statistical parameters good
NESM3 historical-ssp585 (1)	good	good	1.48 (1.34 ... 1.67)	-0.290 (-0.370 ... -0.200)	good
NorESM2-MM historical-ssp585 (1)	good	good	1.90 (1.70 ... 2.12)	-0.250 (-0.350 ... -0.140)	in between reasonable and good, include
UKESM1-0-LL historical-ssp585 (5)	good	good	1.99 (1.90 ... 2.09)	-0.170 (-0.190 ... -0.140)	reasonable, exclude because enough good CMIP5 models
IPSL-CM6A-LR historical-ssp245 (32)	good, from CMIP6	reasonable, from CMIP6	1.69 (1.64 ... 1.75)	-0.220 (-0.250 ... -0.200)	reasonable, observed GMST used, include
GFDL-AM2.5C360 historical (5)	good	good	2.15 (1.99 ... 2.30)	-0.259 (-0.335 ... -0.197)	bad, variability too high
CAM5-1-1degree C20C historical (99)	NA	NA	1.70 (1.68 ... 1.72)	-0.176 (-0.172 ... -0.180)	good, values used with warming level 1.7
MIROC5 C20C historical ()	NA	NA	1.36 (1.33 ... 1.39)	-0.240 (-0.224 ... -0.256)	bad
HadGEM3-A-N216 C20C historical ()	NA	NA	2.00 (1.95 ... 2.05)	-0.240 (-0.218 ... -0.262)	bad

https://doi.org/10.5194/esd-2021-90
Preprint. Discussion started: 12 November 2021


Earth System Dynamics Discussions Open Access EGU

Author contributions. SYP and SFK are the study co-leads, GJvO, FSA, SIS, RV, DC, KLE, JA, RS, MvA and CPM provided analyses and text, MW, WY, SL, DLS, MH, RB and LNL provided data and the synthesis, FL, NG, JT and GAV improved the text, CR, RBS and RH provided figures and FELO initiated the study and contributed to the discussions.

Competing interests. The authors declare no competing interest.

Acknowledgements. We acknowledge the World Climate Research Programme, which, through its Working Group on Coupled Modelling, coordinated and promoted CMIP6. We thank the climate modeling groups for producing and making available their model output, the Earth System Grid Federation (ESGF) for archiving the data and providing access, and the multiple funding agencies who support CMIP6 and ESGF. We thank Urs Beyerle for downloading and curating the CMIP6 data at ETH Zurich. F.L. was supported by the Regional and Global Model Analysis (RGMA) component of the Earth and Environmental System Modeling Program of the U.S. Department of Energy's Office of Biological & Environmental Research (BER) via National Science Foundation IA 1947282.

We would like to express our deep gratitude and respect to Geert Jan van Oldenborgh, co-author of this manuscript, who sadly passed away on 12th October 2021. His outstanding contribution to the science of extreme event attribution and his passion to provide the knowledge, data and analysis tools (https://climexp.knmi.nl/) that are most relevant for society and especially for vulnerable communities has been enormous. We lost an incredible scientist, passionate colleague, and friend.

https://doi.org/10.5194/esd-2021-90
Preprint. Discussion started: 12 November 2021


Earth System Dynamics Discussions Open Access EGU

References

Baldwin, J. W., Dessy, J. B., Vecchi, G. A., and Oppenheimer, M.: Temporally Compound Heat Wave Events and Global Warming: An Emerging Hazard, Earth's Future, 7, 411–427, https://doi.org/https://doi.org/10.1029/2018EF000989, 2019.

Barnes, E. A. and Screen, J. A.: The impact of Arctic warming on the midlatitude jet-stream: Can it? Has it? Will it?, Wiley Interdisciplinary Reviews: Climate Change, 6, 277–286, https://doi.org/10.1002/wcc.337, 2015.

BC Hydro: Not-so well-conditioned: How inefficient A/C use is leaving British Columbians out of pocket in the cold, https://www.google.com/url?q=https://www.bchydro.com/content/dam/BCHydro/customer-portal/documents/news-and-features/bch-ac-report-aug-2020.pdf&sa=D&source=editors&ust=1631004798219000&usg=AOvVaw2Tf3ZD61NG2ahqg_dm7a-k, 2020.

Boucher, O., Servonnat, J., Albright, A. L., Aumont, O., Y., B., Bastriko, V., Bekki, S., Bonnet, R., Bony, S., Bopp, L., Braconnot, P., Brockmann, P., Cadule, P., Caubel, A., Cheru, F., Cozic, A., Cugnet, D., D'Andrea, F., Davini, P., de Lavergne, C., Denvil, S., Deshayes, J., M., D., Ducharne, A., Dufresne, J.-L., Dupont, E., Ethé, C., Fairhead, L., Falletti, L., Foujols, M.-A., Gardoll, S., Gastinea, G., J., G., Grandpeix, J.-Y., Guenet, B., Guez, L., Guilyardi, E., Guimberteau, M., Hauglustaine, D., Hourdin, F., Idelkadi, A., Joussaume, S., Kageyama, M., Khadre-Traoré, A., Khodri, M., Krinner, G., Lebas, N., Levavasseur, G., Lévy, C., Li, L., Lott, F., Lurton, T., Luyssaert, S., G., M., Madeleine, J.-B., Maignan, F., Marchand, M., Marti, O., Mellul, L., Meurdesoif, Y., Mignot, J., Musat, I., Ottlé, C., Peylin, P., Planton, Y., Polcher, J., Rio, C., Rousset, C., Sepulchre, P., Sima, A., Swingedouw, D., Thieblemont, R., Traoré, A., Vancoppenolle, M., Vial, J., Vialard, J., Viovy, N., and Vuichard, N.: Presentation and evaluation of the IPSL-CM6A-LR climate model, J. Adv. Modeling Earth Systems, 12, e2019MS002 010, https://doi.org/10.1029/2019MS002010, 2020.

Brewer, M. C., Mass, C. F., and Potter, B. E.: The West Coast Thermal Trough: Climatology and Synoptic Evolution, Monthly Weather Review, 140, 3820 – 3843, https://doi.org/10.1175/MWR-D-12-00078.1, 2012.

Brewer, M. C., Mass, C. F., and Potter, B. E.: The West Coast Thermal Trough: Mesoscale Evolution and Sensitivity to Terrain and Surface Fluxes, Monthly Weather Review, 141, 2869 – 2896, https://doi.org/10.1175/MWR-D-12-00305.1, 2013.

Bumbaco, K. A., Dello, K. D., and Bond, N. A.: History of Pacific Northwest Heat Waves: Synoptic Pattern and Trends, Journal of Applied Meteorology and Climatology, 52, 1618 – 1631, https://doi.org/10.1175/JAMC-D-12-094.1, 2013.

Chan, D., Vecchi, G., Yang, W., and Huybers, P.: Improved simulation of 19th-and 20th-century North Atlantic hurricane frequency after correcting historical sea surface temperatures, Science advances, 7, https://doi.org/10.1126/sciadv.abg6931, publisher Copyright: © 2021 American Association for the Advancement of Science. All rights reserved., 2021.

Chang, E. K. M., Ma, C.-G., Zheng, C., and Yau, A. M. W.: Observed and projected decrease in Northern Hemisphere extra-tropical cyclone activity in summer and its impacts on maximum temperature, Geophysical Research Letters, 43, 2200–2208, https://doi.org/https://doi.org/10.1002/2016GL068172, 2016.

Christidis, N. and Stott, P. A.: Changes in the geopotential height at 500?hPa under the influence of external climatic forcings, Geophysical Research Letters, 42, 10,798–10,806, https://doi.org/https://doi.org/10.1002/2015GL066669, 2015.

Ciavarella, A., Cotterill, D., Stott, P., Kew, S., Philip, S., van Oldenborgh, G. J., Skålevåg, A., Lorenz, P., Robin, Y., Otto, F., Hauser, M., Seneviratne, S. I., Lehner, F., and Zolina, O.: Prolonged Siberian heat of 2020 almost impossible without human influence, Climatic Change, 166, 9, https://doi.org/10.1007/s10584-021-03052-w, 2021.

Coumou, D., Lehmann, J., and Beckmann, J.: Climate change. The weakening summer circulation in the Northern Hemisphere mid-latitudes, Science (New York, N.Y.), 348, https://doi.org/10.1126/science.1261768, 2015.

https://doi.org/10.5194/esd-2021-90
Preprint. Discussion started: 12 November 2021

Cowan, T., Hegerl, G. C., Schurer, A., Tett, S. F. B., Vautard, R., Yiou, P., Jézéquel, A., Otto, F. E. L., Harrington, L. J., and Ng, B.: Ocean and land forcing of the record-breaking Dust Bowl heatwaves across central United States, Nature Communications, 11, 2870, https://doi.org/10.1038/s41467-020-16676-w, 2020.

D'Ippoliti, D., Michelozzi, P., Marino, C., de'Donato, F., Menne, B., Katsouyanni, K., Kirchmayer, U., Analitis, A., Medina-Ramón, M., Paldy, A., Atkinson, R., Kovats, S., Bisanti, L., Schneider, A., Lefranc, A., Iñiguez, C., and Perucci, C. A.: The impact of heat waves on mortality in 9 European cities: results from the EuroHEAT project, Environmental Health, 9, 37, https://doi.org/10.1186/1476-069X-9-37, 2010.

Donat, M. G., King, A. D., Overpeck, J. T., Alexander, L. V., Durre, I., and Karoly, D. J.: Extraordinary heat during the 1930s US Dust Bowl and associated large-scale conditions, Climate Dynamics, 46, 413–426, https://doi.org/10.1007/s00382-015-2590-5, 2016.

Donat, M. G., Pitman, A. J., and Seneviratne, S. I.: Regional warming of hot extremes accelerated by surface energy fluxes, Geophys. Res. Lett., 44, 7011–7019, https://doi.org/10.1002/2017GL073733, 2017.

Ebi, K. L.: Effective heat action plans: research to interventions, Environmental Research Letters, 14, 122 001, https://doi.org/10.1088/1748-9326/ab5ab0, 2019.

Ebi, K. L., Berry, P., Hayes, K., Boyer, C., Sellers, S., Enright, P. M., and Hess, J. J.: Stress Testing the Capacity of Health Systems to Manage Climate Change-Related Shocks and Stresses, International Journal of Environmental Research and Public Health, 15, https://doi.org/10.3390/ijerph15112370, 2018.

Ebi, K. L., Capon, A., Berry, P., Broderick, C., de Dear, R., Havenith, G., Honda, Y., Kovats, R. S., Ma, W., Malik, A., Morris, N. B., Nybo, L., Seneviratne, S. I., Vanos, J., and Jay, O.: Hot weather and heat extremes: health risks, The Lancet, 398, 698–708, https://doi.org/10.1016/S0140-6736(21)01208-3, 2021.

Eyring, V., Bony, S., Meehl, G. A., Senior, C. A., Stevens, B., Stouffer, R. J., and Taylor, K. E.: Overview of the Coupled Model Intercomparison Project Phase 6 (CMIP6) experimental design and organization, Geoscientific Model Development, 9, 1937–1958, https://doi.org/10.5194/gmd-9-1937-2016, 2016.

Fetterer, F., Knowles, K., Meier, W. N., Savoie, M., and Windnagel, A. K.: Sea Ice Index, Version 3. Ice Extent; Sea Ice Concentration, https://doi.org/10.7265/N5K072F8, accessed 2 July 2021, 2017 (updated daily).

Haarsma, R. J., Selten, F., and van Oldenborgh, G. J.: Anthropogenic changes of the thermal and zonal flow structure over Western Europe and Eastern North Atlantic in CMIP3 and CMIP5 models, Clim. Dyn., 41, 2577–2588, https://doi.org/10.1007/s00382-013-1734-8, 2013.

Haines, A., Kovats, R. S., Campbell-Lendrum, D., and Corvalan, C.: Climate change and human health: impacts, vulnerability, and mitigation., Lancet, 367, 2101–2109, https://doi.org/10.1016/S0140-6736(06)68933-2, erratum in Lancet. 2006 Aug 19;368(9536):646, 2006.

Hall, A., Qu, X., and Neelin, J. D.: Improving predictions of summer climate change in the United States, Geophysical Research Letters, 35, https://doi.org/https://doi.org/10.1029/2007GL032012, 2008.

Hansen, J., Ruedy, R., Sato, M., and Lo, K.: Global Surface Temperature Change, Rev. Geophys., 48, RG4004, https://doi.org/DOI 10.1029/2010RG000345, 2010.

Harvey, B. J., Cook, P., Shaffrey, L. C., and Schiemann, R.: The Response of the Northern Hemisphere Storm Tracks and Jet Streams to Climate Change in the CMIP3, CMIP5, and CMIP6 Climate Models, Journal of Geophysical Research: Atmospheres, 125, e2020JD032 701, https://doi.org/https://doi.org/10.1029/2020JD032701, e2020JD032701 2020JD032701, 2020.

Hauser, M., Orth, R., and Seneviratne, S. I.: Role of soil moisture versus recent climate change for the 2010 heat wave in western Russia, Geophysical Research Letters, 43, 2819–2826, https://doi.org/https://doi.org/10.1002/2016GL068036, 2016.

https://doi.org/10.5194/esd-2021-90
Preprint. Discussion started: 12 November 2021

Hersbach, H., Bell, W., Berrisford, P., Horányi, A., J., M.-S., Nicolas, J., Radu, R., Schepers, D., Simmons, A., Soci, C., and Dee, D.: Global reanalysis: goodbye ERA-Interim, hello ERA5, ECMWF Newsletter, 159, 17–24, https://doi.org/10.21957/vf291hehd7, 2019.

Hess, J. J. and Ebi, K. L.: Iterative management of heat early warning systems in a changing climate, Annals of the New York Academy of Sciences, 1382, 21–30, https://doi.org/https://doi.org/10.1111/nyas.13258, 2016.

Kew, S. F., Philip, S. Y., Hauser, M., Hobbins, M., Wanders, N., van Oldenborgh, G. J., van der Wiel, K., Veldkamp, T. I. E., Kimutai, J., Funk, C., and Otto, F. E. L.: Impact of precipitation and increasing temperatures on drought trends in eastern Africa, Earth System Dynamics, 12, 17–35, https://doi.org/10.5194/esd-12-17-2021, 2021.

Kirchmeier-Young, M. C., Gillett, N. P., Zwiers, F. W., Cannon, A. J., and Anslow, F. S.: Attribution of the Influence of Human-Induced Climate Change on an Extreme Fire Season, Earth's Future, 7, 2–10, https://doi.org/https://doi.org/10.1029/2018EF001050, 2019.

Kornhuber, K. and Tamarin-Brodsky, T.: Future Changes in Northern Hemisphere Summer Weather Persistence Linked to Projected Arctic Warming, Geophysical Research Letters, 48, e2020GL091 603, https://doi.org/https://doi.org/10.1029/2020GL091603, e2020GL091603 2020GL091603, 2021.

Lee, J.-Y., Marotzke, J., Bala, G., Cao, L., Corti, S., Dunne, J., Engelbrecht, F., Fischer, E., Fyfe, J., Jones, C., Maycock, A., Mutemi, J., Ndiaye, O., Panickal, S., and Zhou, T.: Future Global Climate: Scenario-Based Projections and Near-Term Information, in: Climate Change 2021: The Physical Science Basis. Contribution of Working Group I to the Sixth Assessment Report of the Intergovernmental Panel on Climate Change, edited by Masson-Delmotte, V., Zhai, P., Pirani, A., Connors, S., Péan, C., Berger, S., Caud, N., Chen, Y., Goldfarb, L., Gomis, M., Huang, M., Leitzell, K., Lonnoy, E., Matthews, J., Maycock, T., Waterfield, T., Yelekçi, O., Yu, R., and B., Z., chap. 4, Cambridge University Press, in press, 2021.

Lehmann, J., Coumou, D., Frieler, K., Eliseev, A. V., and Levermann, A.: Future changes in extratropical storm tracks and baroclinicity under climate change, Environmental Research Letters, 9, 084 002, https://doi.org/10.1088/1748-9326/9/8/084002, 2014.

Lenssen, N. J. L., Schmidt, G. A., Hansen, J. E., Menne, M. J., Persin, A., Ruedy, R., and Zyss, D.: Improvements in the GISTEMP Uncertainty Model, Journal of Geophysical Research: Atmospheres, 124, 6307–6326, https://doi.org/https://doi.org/10.1029/2018JD029522, 2019.

Lubik, A., McKee, G., Chen, T., and Kosatsky, T.: Municipal Heat Response Planning in British Columbia, Canada, Tech. rep., ENVIRONMENTAL HEALTH SERVICES, BRITISH COLUMBIA CENTER FOR DISEASE CONTROL; NATIONAL COLLABORATING CENTRE FOR ENVIRONMENTAL HEALTH, British Columbia, Canada, 2017.

Menne, M. J., Durre, I., Vose, R. S., Gleason, B. E., and Houston, T. G.: An Overview of the Global Historical Climatology Network-Daily Database, J. Atmos. Oceanic Technol., 29, 897–910, https://doi.org/10.1175/JTECH-D-11-00103.1, 2012.

Mueller, B. and Seneviratne, S. I.: Hot days induced by precipitation deficits at the global scale, Proceedings of the National Academy of Sciences, 109, 12 398–12 403, https://doi.org/10.1073/pnas.1204330109, 2012.

Neale, R. B., Gettelman, A., Park, S., Conley, A. J., Kinnison, D., Marsh, D., Smith, A. K., Vitt, F., Morrison, H., Cameron-smith, P., Collins, W. D., Iacono, M. J., Easter, R. C., Liu, X., Taylor, M. A., chieh Chen, C., Lauritzen, P. H., Williamson, D. L., Garcia, R., francois Lamarque, J., Mills, M., Tilmes, S., Ghan, S. J., Rasch, P. J., and Meteorology, M.: Description of the NCAR Community Atmosphere Model (CAM 5.0), Tech. Note NCAR/TN-486+STR, Natl. Cent. for Atmos, in: 6of7 ZHAO ET AL.: AEROSOL FIE SIMULATED BY CAMS L08806, pp. 2009–038 451, 2010.

O'Neill, B. C., Tebaldi, C., van Vuuren, D. P., Eyring, V., Friedlingstein, P., Hurtt, G., Knutti, R., Kriegler, E., Lamarque, J.-F., Lowe, J., Meehl, G. A., Moss, R., Riahi, K., and Sanderson, B. M.: The Scenario Model Intercomparison Project (ScenarioMIP) for CMIP6, Geoscientific Model Development, 9, 3461–3482, https://doi.org/10.5194/gmd-9-3461-2016, 2016.

https://doi.org/10.5194/esd-2021-90
Preprint. Discussion started: 12 November 2021

Pfleiderer, P., Schleussner, C.-F., Kornhuber, K., and Coumou, D.: Summer weather becomes more persistent in a 2 °C world, Nature Climate Change, 9, 666–671, https://doi.org/10.1038/s41558-019-0555-0, 2019.

Philip, S. Y., Kew, S. F., van Oldenborgh, G. J., Otto, F. E. L., Vautard, R., van der Wiel, K., King, A. D., Lott, F. C., Arrighi, J., Singh, R. P., and van Aalst, M. K.: A protocol for probabilistic extreme event attribution analyses, Advances in Statistical Climatology, Meteorology and Oceanography, 6, 177–203, https://doi.org/10.5194/ascmo-6-177-2020, 2020.

Routson, C. C., McKay, N. P., Kaufman, D. S., Erb, M. P., Goosse, H., Shuman, B. N., Rodysill, J. R., and Ault, T.: Mid-latitude net precipitation decreased with Arctic warming during the Holocene, Nature, 568, 83–87, https://doi.org/10.1038/s41586-019-1060-3, 2019.

Seneviratne, S. I., Corti, T., Davin, E. L., Hirschi, M., Jaeger, E. B., Lehner, I., Orlowsky, B., and Teuling, A. J.: Investigating soil moisture?climate interactions in a changing climate: A review, Earth-Science Reviews, 99, 125–161, https://doi.org/https://doi.org/10.1016/j.earscirev.2010.02.004, 2010.

Singh, R., Arrighi, J., Jjemba, E., Strachan, K., Spires, M., and Kadihasanoglu, A.: Heatwave Guide for Cities, Tech. rep., Red Cross Red Crescent Climate Centre., 2019.

Skamarock, C., Klemp, B., Dudhia, J., Gill, O., Liu, Z., Berner, J., Wang, W., Powers, G., Duda, G., Barker, D., and yu Huang, X.: A Description of the Advanced Research WRF Model Version 4, Tech. rep., NCAR, tech. Note NCAR/TN-556+STR, 145 pp, 2019.

Stewart, R. E., Betancourt, D., Davies, J. B., Harford, D., Klein, Y., Lannigan, R., Mortsch, L., O'Connell, E., Tang, K., and Whitfield, P. H.: A multi-perspective examination of heat waves affecting Metro Vancouver: now into the future, Natural Hazards, 87, 791–815, https://doi.org/10.1007/s11069-017-2793-7, 2017.

Stone, D. A., Christidis, N., Folland, C., Perkins-Kirkpatrick, S., Perlwitz, J., Shiogama, H., Wehner, M. F., Wolski, P., Cholia, S., Krishnan, H., Murray, D., Angélil, O., Beyerle, U., Ciavarella, A., Dittus, A., Quan, X.-W., and Tadross, M.: Experiment design of the International CLIVAR C20C+ Detection and Attribution project, Weather and Climate Extremes, 24, 100 206, https://doi.org/https://doi.org/10.1016/j.wace.2019.100206, 2019.

Stringfellow, M. and Wagle, D.: The Economics of Homelessness in Seattle and King County, McKinsey & Company, retrieved from: https://www.mckinsey.com/featured-insights/future-of-cities/the-economics-of-homelessness-in-seattle-and-king-county. (Accessed on: July 4, 2021), 2018.

Tang, Q., Zhang, X., and Francis, J. A.: Extreme summer weather in northern mid-latitudes linked to a vanishing cryosphere, Nature Climate Change, 4, 45–50, https://doi.org/10.1038/nclimate2065, 2014.

Taylor, K. E., Stouffer, R. J., and Meehl, G. A.: An Overview of CMIP5 and the Experiment Design, Bull. Amer. Met. Soc., 93, 485–498, https://doi.org/10.1175/BAMS-D-11-00094.1, 2011.

Thiery, W., Davin, E. L., Lawrence, D. M., Hirsch, A. L., Hauser, M., and Seneviratne, S. I.: Present-day irrigation mitigates heat extremes, Journal of Geophysical Research: Atmospheres, 122, 1403–1422, https://doi.org/10.1002/2016JD025740, 2017.

U.S. Census Bureau: American Housing Survey (AHS), retrieved from: https://www.census.gov/programs-surveys/ahs/data/interactive/ahstablecreator.html, 2019.

van Oldenborgh, G. J., van der Wiel, K., Kew, S., Philip, S., Otto, F., Vautard, R., King, A., Lott, F., Arrighi, J., Singh, R., and van Aalst, M.: Pathways and pitfalls in extreme event attribution, Climatic Change, 166, 13, https://doi.org/10.1007/s10584-021-03071-7, 2021.

Vautard, R., van Aalst, M. K., Boucher, O., Drouin, A., Haustein, K., Kreienkamp, F., van Oldenborgh, G. J., Otto, F. E. L., Ribes, A., Robin, Y., Schneider, M., Soubeyroux, J.-M., Stott, P. A., Seneviratne, S. I., Vogel, M. M., and Wehner, M. F.: Human contribution to the record-breaking June and July 2019 heat waves in Western Europe, Environ. Res. Lett., 15, 094 077, https://doi.org/10.1088/1748-9326/aba3d4, 2020.

https://doi.org/10.5194/esd-2021-90
Preprint. Discussion started: 12 November 2021

Vavrus, S.: The Influence of Arctic Amplification on Mid-latitude Weather and Climate, Current Climate Change Reports, 4, https://doi.org/10.1007/s40641-018-0105-2, 2018.

Vecchi, G. A., Delworth, T., Gudgel, R., Kapnick, S., Rosati, A., Wittenberg, A. T., Zeng, F., Anderson, W., Balaji, V., Dixon, K., et al.: On the seasonal forecasting of regional tropical cyclone activity, J. Climate, 27, 7994–8016, https://doi.org/10.1175/JCLI-D-14-00158.1, 2014.

Vincent, L. A., Hartwell, M. M., and Wang, X. L.: A Third Generation of Homogenized Temperature for Trend Analysis and Monitoring Changes in Canada?s Climate, Atmosphere-Ocean, 58, 173–191, https://doi.org/10.1080/07055900.2020.1765728, 2020.

Wehrli, K., Guillod, B. P., Hauser, M., Leclair, M., and Seneviratne, S. I.: Identifying Key Driving Processes of Major Recent Heat Waves, Journal of Geophysical Research: Atmospheres, 124, 11 746–11 765, https://doi.org/https://doi.org/10.1029/2019JD030635, 2019.

Yang, W., Hsieh, T.-L., and Vecchi, G. A.: Hurricane annual cycle controlled by both seeds and genesis probability, Proceedings of the National Academy of Sciences, 118, https://doi.org/10.1073/pnas.2108397118, 2021.